REPORT DOCUMENTATION PAGE

Form Approved OMB NO. 0704-0188

1. REPORT DATE (DD-MM-YYYY)	2. REPORT TYPE	3. DATES COVERED (From - To)
04-08-2015	Final Report	1-Jun-2008 - 31-Dec-2014

4. TITLE AND SUBTITLE
DNA TRANSPORT IN NANOPARTICLE POROUS-WALL NANOCHANNELS

5a. CONTRACT NUMBER
W911NF-08-1-0214

5b. GRANT NUMBER

5c. PROGRAM ELEMENT NUMBER
622622

6. AUTHORS
S. R. J. Brueck

5d. PROJECT NUMBER

5e. TASK NUMBER

5f. WORK UNIT NUMBER

7. PERFORMING ORGANIZATION NAMES AND ADDRESSES
University of New Mexico Albuquerque
1700 Lomas Blvd. NE, Suite 2200, MSC01 1247
1 University of New Mexico
Albuquerque, NM 87131 -0001

8. PERFORMING ORGANIZATION REPORT NUMBER

9. SPONSORING/MONITORING AGENCY NAME(S) AND ADDRESS (ES)
U.S. Army Research Office
P.O. Box 12211
Research Triangle Park, NC 27709-2211

10. SPONSOR/MONITOR'S ACRONYM(S)
ARO

11. SPONSOR/MONITOR'S REPORT NUMBER(S)
54630-EL-H.6

12. DISTRIBUTION AVAILIBILITY STATEMENT
Approved for Public Release; Distribution Unlimited

13. SUPPLEMENTARY NOTES
The views, opinions and/or findings contained in this report are those of the author(s) and should not contrued as an official Department of the Army position, policy or decision, unless so designated by other documentation.

14. ABSTRACT
New types of chips were fabricated based on nanochannel structures with porous walls and roofs for a variety of investigations of nanofluidic properties, electrophoresis, DNA stretching properties and transport in nanostructures, influence of electric field and dye bonding on the behavior of DNA molecules in the nanochannels. Advantages of the structures are demonstrated for the future investigations of manipulation with DNA and other biomolecules.

15. SUBJECT TERMS
nanochannels, porous media, DNA transport

16. SECURITY CLASSIFICATION OF:			17. LIMITATION OF ABSTRACT	15. NUMBER OF PAGES	19a. NAME OF RESPONSIBLE PERSON
a. REPORT	b. ABSTRACT	c. THIS PAGE			Steven Brueck
UU	UU	UU	UU		19b. TELEPHONE NUMBER 505-272-7800

Report Title

DNA TRANSPORT IN NANOPARTICLE POROUS-WALL NANOCHANNELS

ABSTRACT

New types of chips were fabricated based on nanochannel structures with porous walls and roofs for a variety of investigations of nanofluidic properties, electrophoresis, DNA stretching properties and transport in nanostructures, influence of electric field and dye bonding on the behavior of DNA molecules in the nanochannels. Advantages of the structures are demonstrated for the future investigations of manipulation with DNA and other biomolecules.

Enter List of papers submitted or published that acknowledge ARO support from the start of the project to the date of this printing. List the papers, including journal references, in the following categories:

(a) Papers published in peer-reviewed journals (N/A for none)

Received		Paper
07/02/2013	1.00	Deying Xia, Jingyu Zhang, Xiang He, S. R. J. Brueck. Fabrication of three-dimensional photonic crystal structures by interferometric lithography and nanoparticle self-assembly, Applied Physics Letters, (08 2008): 71105. doi: 10.1063/1.2971202
07/02/2013	4.00	Deying Xia, Zahyun Ku, S. C. Lee, S. R. J. Brueck. Nanostructures and Functional Materials Fabricated by Interferometric Lithography, Advanced Materials, (01 2011): 147. doi: 10.1002/adma.201001856
07/13/2015	2.00	Anthony L. Garcia, Youn-Jin Oh, Gabriel P. Lopez, Steven R. J. Brueck, Cornelius F. Ivory, Sang M. Han, Dimiter N. Petsev. Effect of wall–molecule interactions on electrokinetic transport of charged molecules in nanofluidic channels during FET flow control, Lab on a Chip, (2009): 1601. doi: 10.1039/b901382m
07/13/2015	3.00	E. R. Brown, Edgar. A. Mendoza, Deying Xia, S. R. J. Brueck. Narrow THz Spectral Signatures Through an RNA Solution in Nanofluidic Channels, IEEE Sensors Journal, (03 2010): 755. doi: 10.1109/JSEN.2009.2039522
07/13/2015	5.00	S. C. Lee, L. R. Dawson, S. H. Huang, S. R. J. Brueck. Lithography-free Nanoscale Patterned Growth of GaAs on Si(001) with Sub-100-nm Silica Nanoparticles by Molecular Beam Epitaxy, Crystal Growth & Design, (09 2011): 3673. doi: 10.1021/cg101363q
TOTAL:	**5**	

Number of Papers published in peer-reviewed journals:

(b) Papers published in non-peer-reviewed journals (N/A for none)

Received Paper

TOTAL:

Number of Papers published in non peer-reviewed journals:

(c) Presentations

Number of Presentations:

Non Peer-Reviewed Conference Proceeding publications (other than abstracts):

Received Paper

TOTAL:

Number of Non Peer-Reviewed Conference Proceeding publications (other than abstracts):

Peer-Reviewed Conference Proceeding publications (other than abstracts):

Received Paper

TOTAL:

Number of Peer-Reviewed Conference Proceeding publications (other than abstracts):

(d) Manuscripts

Received Paper

TOTAL:

Number of Manuscripts:

Books

Received Book

TOTAL:

Received Book Chapter

TOTAL:

Patents Submitted

Patents Awarded

Awards

Graduate Students

NAME	PERCENT_SUPPORTED

FTE Equivalent:
Total Number:

Names of Post Doctorates

NAME	PERCENT_SUPPORTED

FTE Equivalent:
Total Number:

Names of Faculty Supported

NAME	PERCENT_SUPPORTED

FTE Equivalent:
Total Number:

Names of Under Graduate students supported

NAME	PERCENT_SUPPORTED

FTE Equivalent:
Total Number:

Student Metrics

This section only applies to graduating undergraduates supported by this agreement in this reporting period

The number of undergraduates funded by this agreement who graduated during this period: .....

The number of undergraduates funded by this agreement who graduated during this period with a degree in science, mathematics, engineering, or technology fields:.....

The number of undergraduates funded by your agreement who graduated during this period and will continue to pursue a graduate or Ph.D. degree in science, mathematics, engineering, or technology fields:.....

Number of graduating undergraduates who achieved a 3.5 GPA to 4.0 (4.0 max scale):.....

Number of graduating undergraduates funded by a DoD funded Center of Excellence grant for Education, Research and Engineering:.....

The number of undergraduates funded by your agreement who graduated during this period and intend to work for the Department of Defense .....

The number of undergraduates funded by your agreement who graduated during this period and will receive scholarships or fellowships for further studies in science, mathematics, engineering or technology fields: .....

Names of Personnel receiving masters degrees

NAME

Total Number:

Names of personnel receiving PHDs

NAME

Total Number:

Names of other research staff

NAME PERCENT_SUPPORTED

FTE Equivalent:
Total Number:

Sub Contractors (DD882)

Inventions (DD882)

5 **Fabrication of Enclosed Nanochannels using Silica Nanoparticles**

Patent Filed in US? (5d-1) Y

Patent Filed in Foreign Countries? (5d-2) N

Was the assignment forwarded to the contracting officer? (5e) N

Foreign Countries of application (5g-2):

5a: Steven R. J. Brueck

5f-1a: University of New Mexico

5f-c: 1 University of New Mexico

Albuquerque NM 87131

5a: Deying Xia

5f-1a: University of New Mexico

5f-c: 1 University of New Mexico

Albuquerque NM 87131

5 **Integrated Affinity Microcolumns and Affinity Capillary Electrophoresis**

Patent Filed in US? (5d-1) Y

Patent Filed in Foreign Countries? (5d-2) N

Was the assignment forwarded to the contracting officer? (5e) N

Foreign Countries of application (5g-2):

5a: Linnea K. Ista

5f-1a: University of New Mexico

5f-c: 1 University of New Mexico

Albuquerque NM 87131

5a: M. Bore

5f-1a: University of New Mexico

5f-c: 1 University of New Mexico

Albuquerque NM 87131

5a: Steven R. J. Brueck

5f-1a: University of New Mexico

5f-c: 1 University of New Mexico

Albuquerque NM 87131

5a: Gabriel P. Lopez

5f-1a: University of New Mexico

5f-c: 1 University of New Mexico

Albuquerque NM 87131

5a: A. E. Lara

5f-1a: University of New Mexico

5f-c: 1 University of New Mexico

Albuquerque NM 87131

5 **Nanofluidics for bioseparation and analysis**

Patent Filed in US? (5d-1) Y

Patent Filed in Foreign Countries? (5d-2) N

Was the assignment forwarded to the contracting officer? (5e) N

Foreign Countries of application (5g-2):

5a: Gabriel P. Lopez

5f-1a: University of New Mexico

5f-c: 1 University of New Mexico

Albuquerque NM 87131

5a: Dimiter N. Petsev

5f-1a: University of New Mexico

5f-c: 1 University of New Mexico

Albuquerque NM 87131

5a: Steven R. J. Brueck

5f-1a: University of New Mexico

5f-c: 1 University of New Mexico

Albuquerque NM 87131

5a: Sang M. Han

5f-1a: University of New Mexico

5f-c: 1 University of New Mexico

Albuquerque NM 87131

5a: Cornelius F. Ivory

5f-1a: Washington State University

5f-c:

Pullman WA 99164

5 **Nanostructured Separation and Analysis Devices for Biological Membranes**

Patent Filed in US? (5d-1) Y

Patent Filed in Foreign Countries? (5d-2) N

Was the assignment forwarded to the contracting officer? (5e) N

Foreign Countries of application (5g-2):

5a: Steven R. J. Brueck

5f-1a: University of New Mexico

5f-c: 1 University of New Mexico

Albuquerque NM 87131

5a: Gabriel P. Lopez
5f-1a: University of New Mexico
5f-c: 1 University of New Mexico
Albuquerque NM 87131
5a: Linnea K. Ista
5f-1a: University of New Mexico
5f-c: 1 University of New Mexico
Albuquerque NM 87131

Scientific Progress

see attachment

Technology Transfer

DNA TRANSPORT IN NANOPARTICLE POROUS-WALL NANOCHANNELS

Center for High Technology Materials and Departments of Physics and Astronomy and Electrical and Computer Engineering, University of New Mexico, 1313 Goddard SE, Albuquerque, New Mexico, USA

Abstract

New types of chips were fabricated based on nanochannel structures with porous walls and roofs for a variety of investigations of nanofluidic properties, electrophoresis, DNA stretching properties and transport in nanostructures, influence of electric field and dye bonding on the behavior of DNA molecules in the nanochannels. Advantages of the structures are demonstrated for the future investigations of manipulation with DNA and other biomolecules.

1. Fabrication of chips with channels and porous walls.

The goal of the project is study DNA movement and extension in 1D channels with porous walls. It is obvious from the great amount of previous reports that interests on Lab-on a Chip systems or micro- or nanofluidic systems for analyzing biological or chemical samples have tremendously increased in the last years [1,2]. Micro- and nanochannel structures are used to separate, manipulate, and elongate DNA [3-8]. There are a lot of fabrication techniques for nanofluidic channel devices [9-11]. Compared to previous fabrication approaches, our method has the advantages of ease of fabrication and, importantly for the first time, the provision of interconnected porous structures.

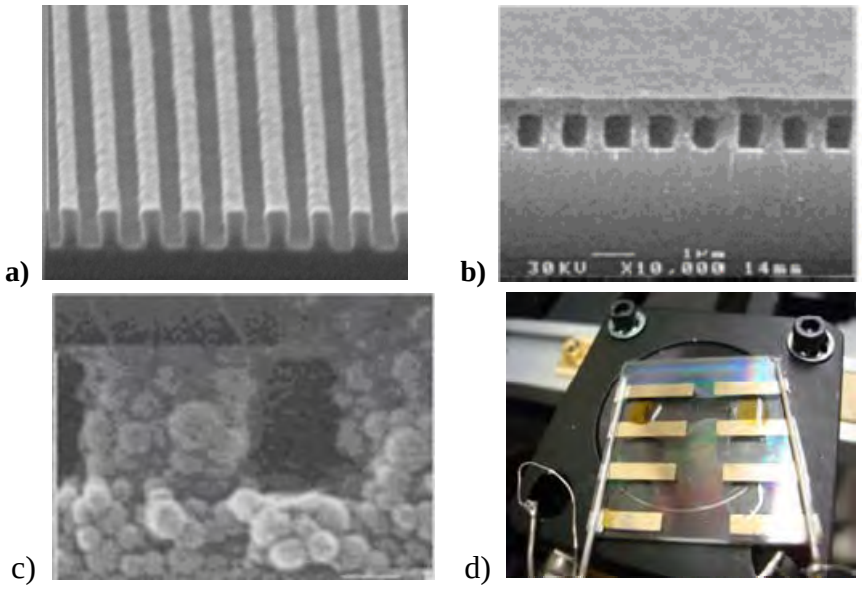

Figure 1. (a) Photoresist pattern, (b) One-dimensional enclosed channels with silica particles, (c) magnified SEM image of channels walls formed by 50 nm silica particles, (d) Nanochannel sample with wells and contacts for applying an electric potential across the channels

We investigated DNA transport in 1D porous nanochannel structures, using capillary action (hydrophilic surface tension) and electrophoresis as the driving forces. The nanochannels were fabricated starting with photoresist patterns on quartz base defined by interferometric

lithography which was used as a soft template (Fig 1 (a)) around which silica nanoparticles were self-assembled by spin coating with a colloidal nanoparticle suspension (Fig 1 (b)) [12,13]. The final fabrication step was an 800° C bake in an air ambient to burn out the photoresist and sinter the nanoparticles. The result was a parallel array of 100- to 500-nm wide nanochannels with porous walls and roofs fabricated from silica nanoparticles of 50-nm diameter (Fig. 1 (c)) [14]. Next, we etch wells at the ends of the channels by reactive ion etching to allow for filling of liquid samples into the channels and add contacts by chrome and gold deposition at the bottom of the wells for the application of an electric potential (Fig 1(d)). There is a strong enhancement of the concentration in the nanochannels compared to a bulk solution which provides a unique medium for spectroscopic investigations. Additionally, porous regions could be interspersed in the channels providing a unique separation medium with multiple channel-porous medium interfaces

2. DNA reaction on applied electric field in nanochannels.

DNA solution was applied to one side and a buffer solution to the other to fill the area between wells and provide conductivity through the channels (Fig 2(a)). DNA transport was monitored by laser induced fluorescence through the transparent silica nanoparticle roof. The set-up with pumping laser beam to provide excitation of YoYo-1 dye attached to DNA molecules and allow investigation of the impact of an applied electric field on the kinetics of stretched DNA molecules is shown in Fig 2(b). Two types of DNA are used: a comparatively large DNA strand, lambda-phage (~49,000 bp), and a low molecular weight (LMW) strand (~ 200 bp). The kinetics of DNA molecules is recorded by a CCD camera and the separate frames are shown in this report.

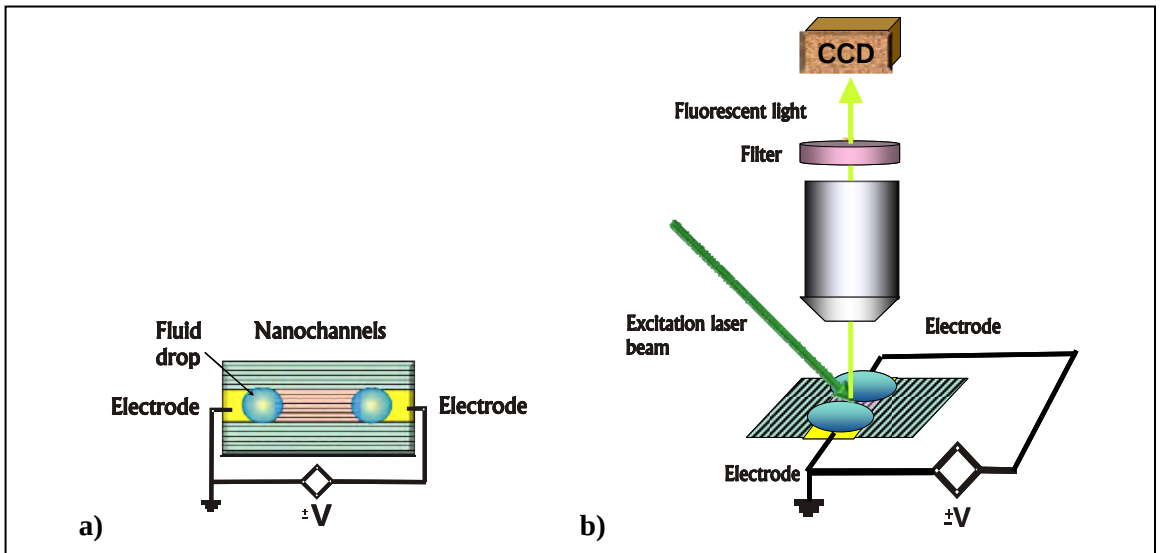

Figure 2. (a) Nanochannel sample with DNA solution penetrated between wells with contacts, (b) set-up with nanochannel sample for investigation of the impact of the applied electric field.

The results of the experiments with an applied electric field demonstrated movement of the negatively charged Lambda and LMW DNA towards the positive contact. Observations of

the drops in the wells (while the buffer solution was on the other side) showed that applied electric field caused Lambda DNA movement to the edge of the drop against the electric field Fig 3(a) and fast penetration through the channels as well as DNA molecule accumulation on the edge of the drop Fig 3(b). The opposite electric field initiated the movement of the band of accumulated DNA from the edge of the drop towards a connected electrode. Pictures in Fig 3(c,d,e) show the DNA band location in the drop in ~ 0.1 s intervals after applying the electric field.

Some DNA molecules appear stuck in blocked channels and accumulated (Fig 4(a)). Applied electric field in the direction of DNA movement stretched the molecules towards the positive electrode Fig 4(b).The electric field in the opposite direction compresses DNA at the obstacles and sometimes allowed them to penetrate through the obstacle (Fig 4(c)). The same experiment was done with the DNA solution on the right side of the sample and buffer solution on the left. DNA molecules stuck at obstacles on the right side (Fig 4(d)), were compressed when positive potential was applied to the left (Fig 4(e)) and stretched by the field with positive potential applied to the right (Fig 4(f)).

The dependence of DNA length and distance from an obstacle in time is shown in Fig. 5(a). DNA flow is from left to right. Change of the potential applied to the right electrode at the same time is shown in Fig. 5(b). Change of DNA length is shown in Fig. 5(c). The electric field applied at the same direction as DNA flow stretched the molecules (-3V stretches from 7 to 10um). If the molecule was released and began to move then length of the molecule was decreased (8 um). The increasing potential kept the molecule movement in the same direction. The potential change to opposite caused the molecule length increasing (12um) and switching direction of the movement. Then the molecule was compressed to 2 um at the obstacle. However, DNA extension depends not only on applied potential and polarity but on time of the potential impact, distance from electrodes, wetability of a sample, quality of channels, and evaporation from the surface. Therefore the estimation of DNA extension should include all these parameters,

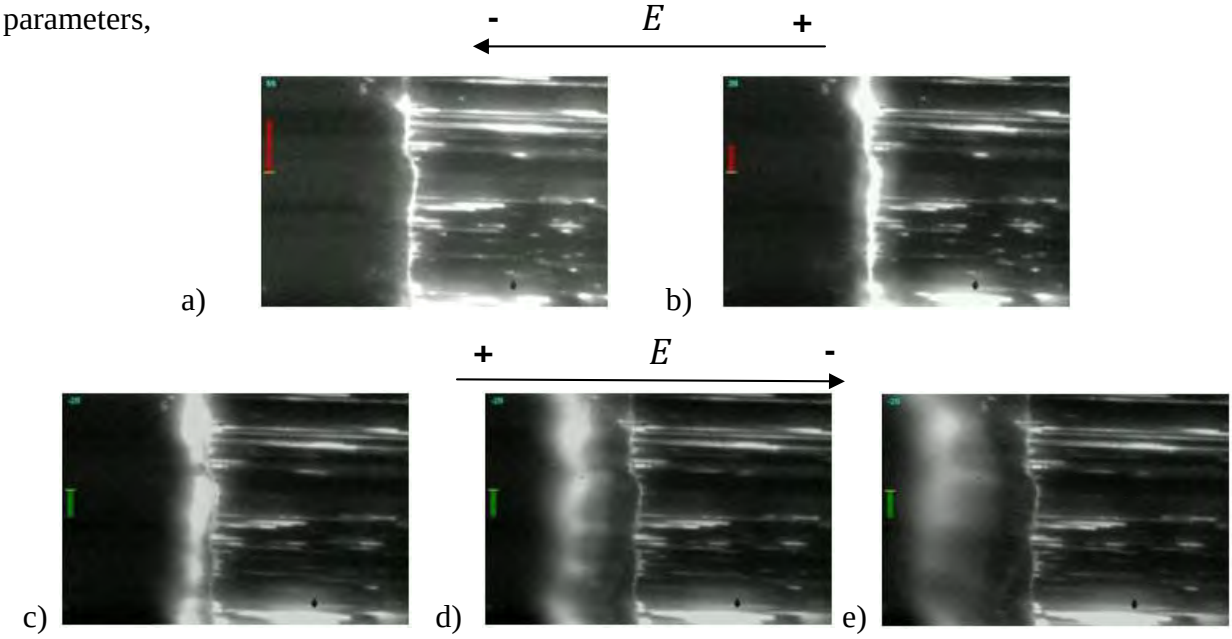

Figure 3. (a) DNA movement to the drop edge, (b) DNA accumulation on the drop edge;

DNA band location in (c) 0.1 s, (c) 0.2 s, (c) 0.3 s after applying the electric field.

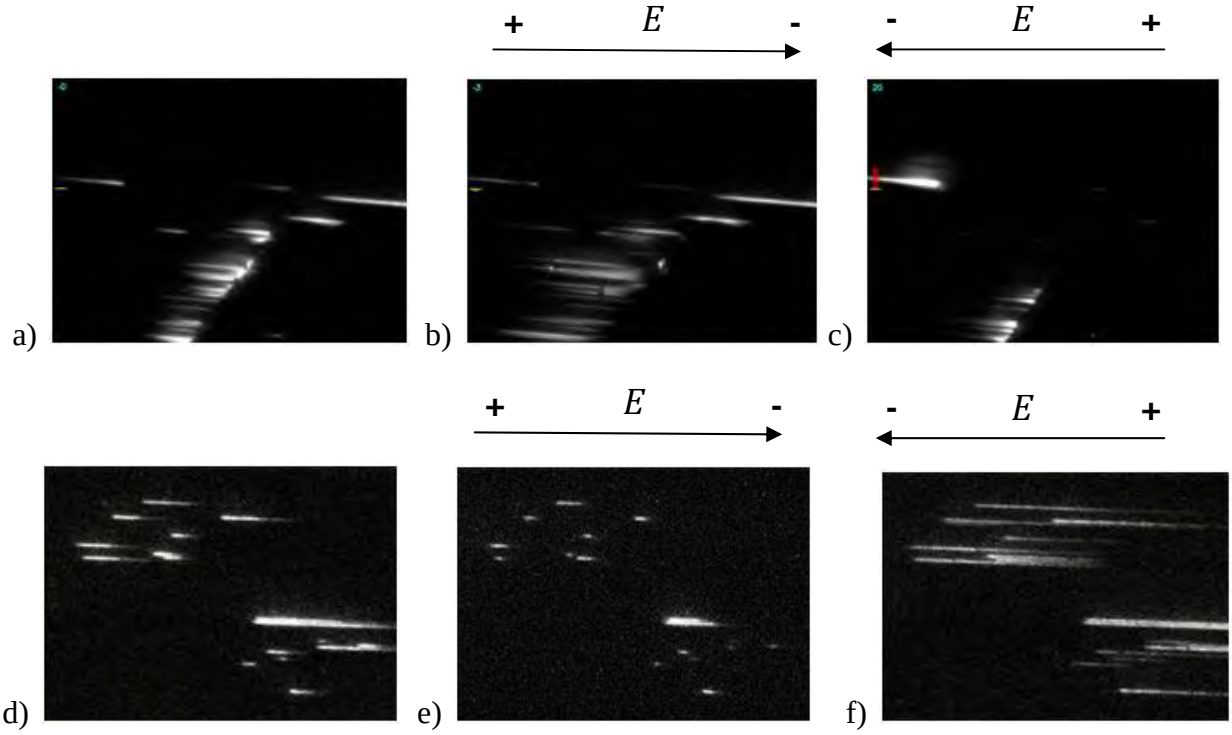

Figure 4. (a) Fluorescent image of DNA flow from left to right in 1D channels: (b) DNA extension with positive potential applied to the right well, (c) DNA extension with positive potential applied to the left well, (d) Fluorescent image of DNA flow from right to left in 1D channels: (e) DNA extension with positive potential applied to the right well, (f) DNA extension with positive potential applied to the left well.

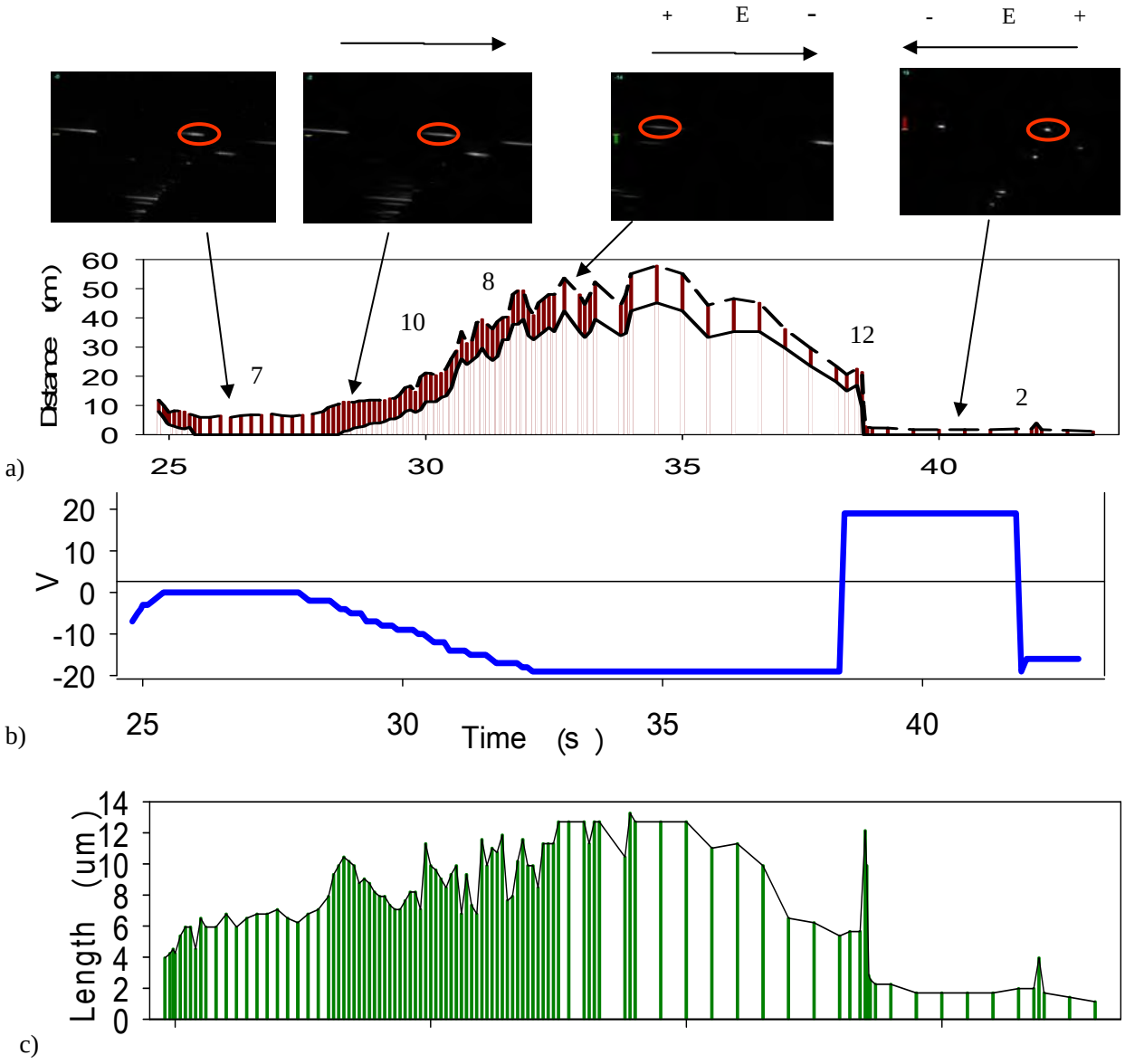

Figure 5. a) DNA length and distance from the obstacle in time, b) potential change in time, c) DNA length change in tine

3.. Chips with channels and porous media.

The next group of experiments was conducted using samples with channels on one side and porous media on the other side (Fig. 6(a)). The porous between 50 nm particles was estimated to be ~ 15 nm. DNA solution came through the channels and stopped at the porous media (Fig 5(b)). In a few minutes penetration through porous began to take place (Fig 6(c)).

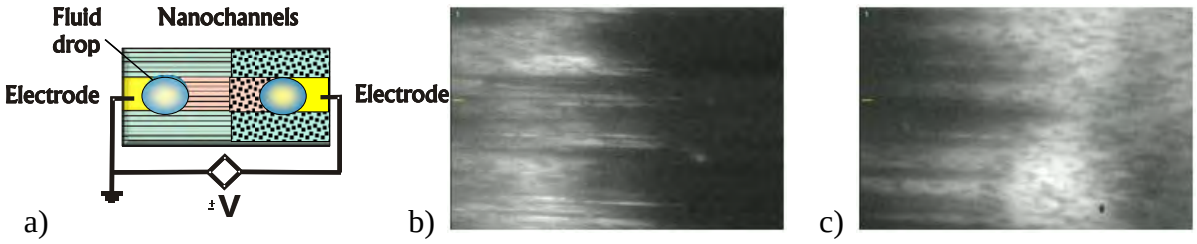

Figure 6. (a) Sample with nanochannels on the left and porous media on the right, (b) DNA accumulation on media separation, (c) DNA penetration in porous

An applied electric field with positive potential on the left caused DNA accumulation at the drop edge in porous media and DNA penetration through pores. Pictures in Fig 7(a,b,c) are taken with an interval of 0.4 s. The bright spots in the porous media were produced by the accumulation of DNA in damaged regions. The opposite electric field led to an accumulated DNA band movement from the edge. Pictures in Fig 76(d,e,f) are taken in 0.6 s intervals. Increasing the electric field with positive potential on the left enhanced the DNA penetration into the porous media also drying the drop as well (Fig 7(g,h,i)).

The electric field with positive potential on the right provided fast penetration of DNA from channels to the porous media (Fig 8(a)) and DNA compression (Fig 8(b)). The opposite electric field almost stopped penetration and probably stretched DNA molecules to the left. The same experimental results are shown for another area with group of channels filled with DNA solution in Fig 8(c,d).

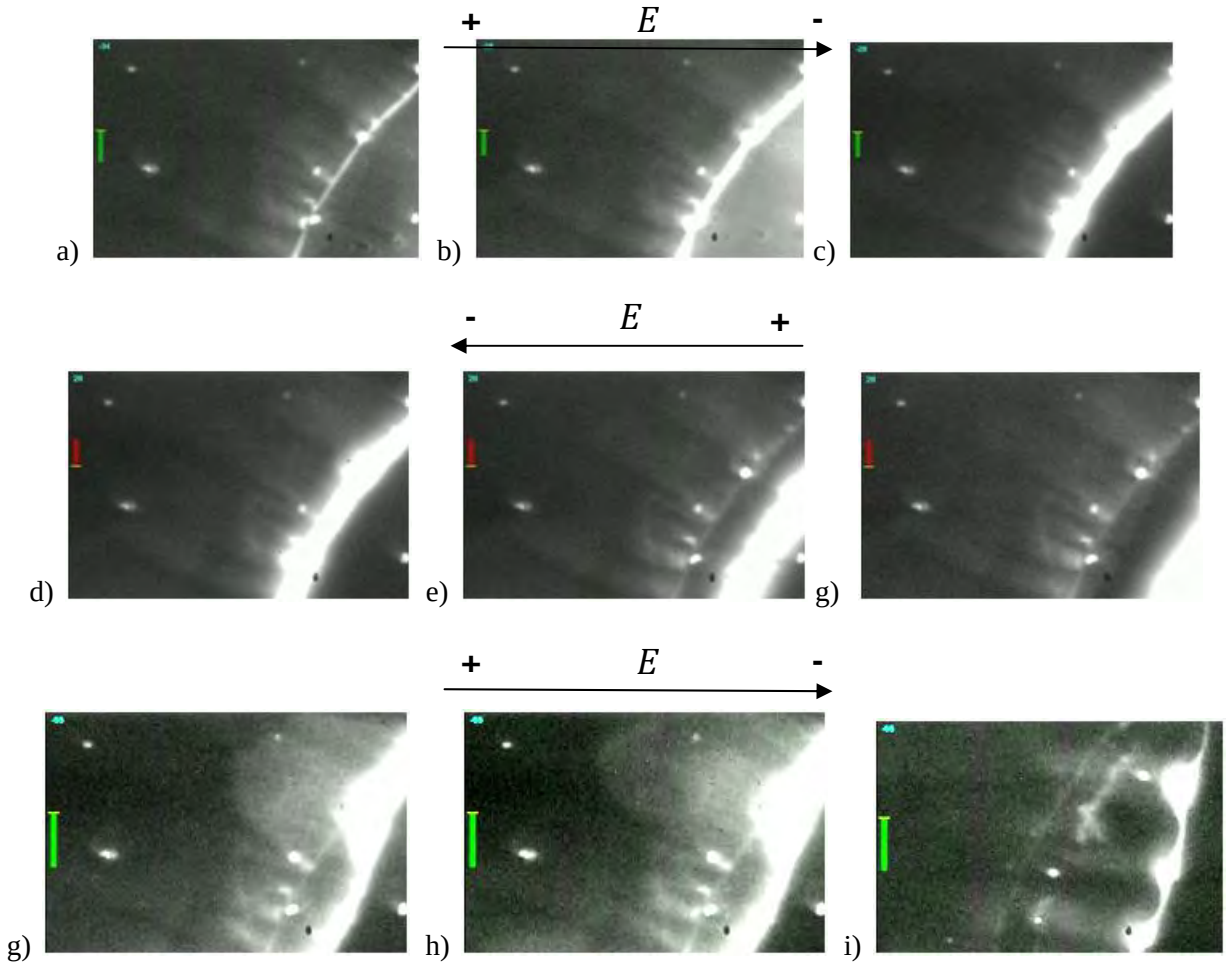

Figure 7. (a) DNA movement to the drop edge; (b) DNA accumulation on the drop edge in 0.4 s, (c) in 0.8 s. DNA band location in (d) 0.6 s, (e) 1.2 s, (f) 1.8 s after applying the electric field. (g,h,i) DNA penetration into porous media.

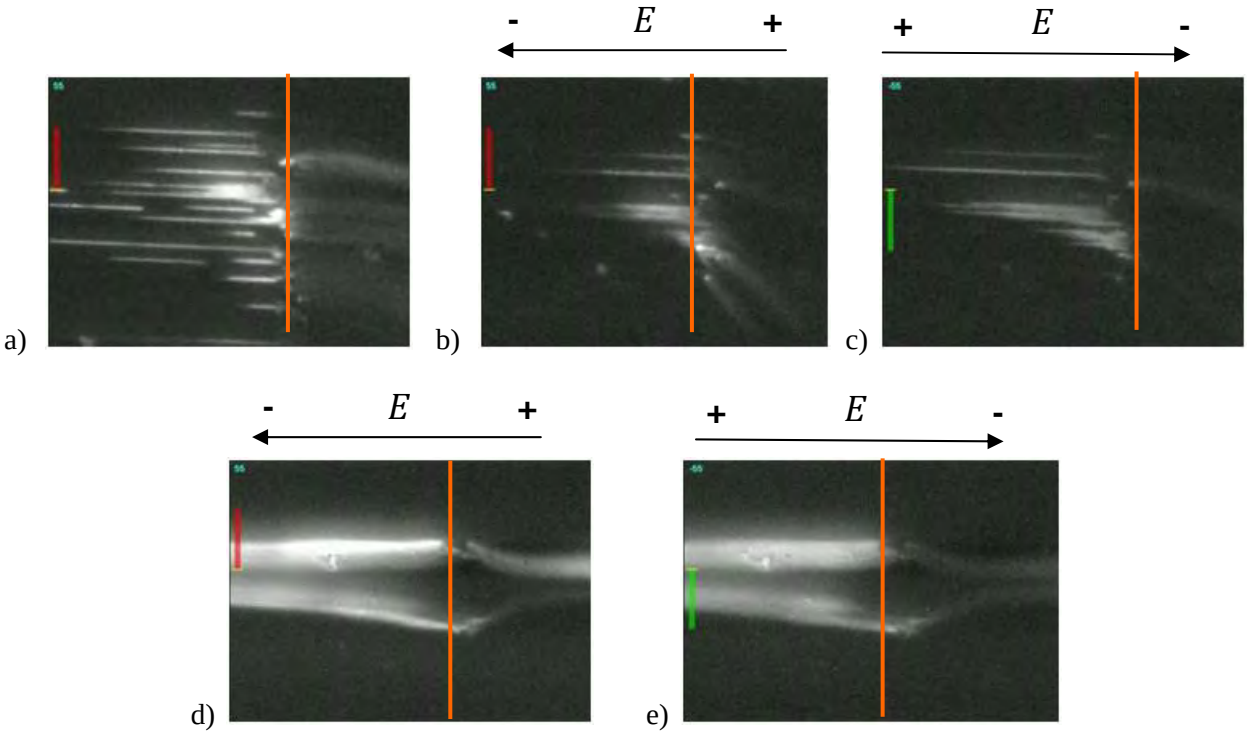

Figure 8. (a) DNA accumulation at media separation and penetration to porous, (b) DNA compression and penetration to porous media stired up by the electric field, (c) decreasing penetration and stretching DNA. Another area (d) increasing penetration, (e) decreasing penetration. (Media separation is shown by the orange line)

4. Penetration of DNA drops through porous walls.

Experiments with drops on the surface of the samples demonstrated a difference in penetration of DNA molecules (dyed with YOYO-1) with different size through porous media. Lambda DNA penetrated through the roof much faster (~5 min) and moved through the channels (Fig 9 (a)). LMW DNA penetration took around 15 min. LMW were located more in porous media than in the channels (Fig 9 (b)). However, the ration of DNA concentration to dye should be taken in consideration because it has a huge impact on molecules penetration.

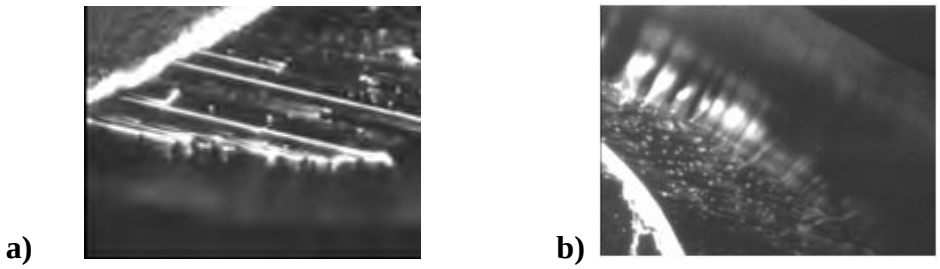

Figure 9. Penetration of fluorescent DNA through the porous roof to the channels: (a) Lambda DNA, (b) LMW DNA

We observed a fluorescence of a drop of YOYO-1 dye on the porous roof of nanochannel structure but there was no fluorescence in the nanochannels (Fig 10 (a)). The recommended ratio of concentrations (1 µl of YOYO-1, 13.4 µl of lambda DNA dye and 1000 µl of TBE solution) results in fluorescent drop and appearance of yellow clusters which concentrate at the drop border (Fig 10 (b)). Decreasing of the dye concentration ratio by twice (0.5 µl of YOYO-1 dye, 13.4 µl of lambda DNA, 1000 µl of TBE) results in decreasing of fluorescence intensity in the drop (Fig 10 (c)). Next reduction of dye to 0.25 µl at the same concentration of Lambda DNA allows us to see fluorescence in nanochannels (Fig 10 (d)). The intensity of the fluorescent in nanochanels increases with dye concentration reduction to 0.125 µl (Fig 2 (e)), but further reduction results in fluorescence decreasing: 0.063 µl YOYO-1 (Fig 10 (f)), 0.032 µl YOYO-1 (Fig 10 (g)), 0.016 µl of (Fig 10 (h)). Note, that the border around the drop disappears with dye reduction. This experiment allows us to choose ratio which gives maximum fluorescent intensity for the particular dye in porous nanochannels. The area with nanochannels was selected from pictures shown on Fig.10 and histograms of intensity distribution were obtained.

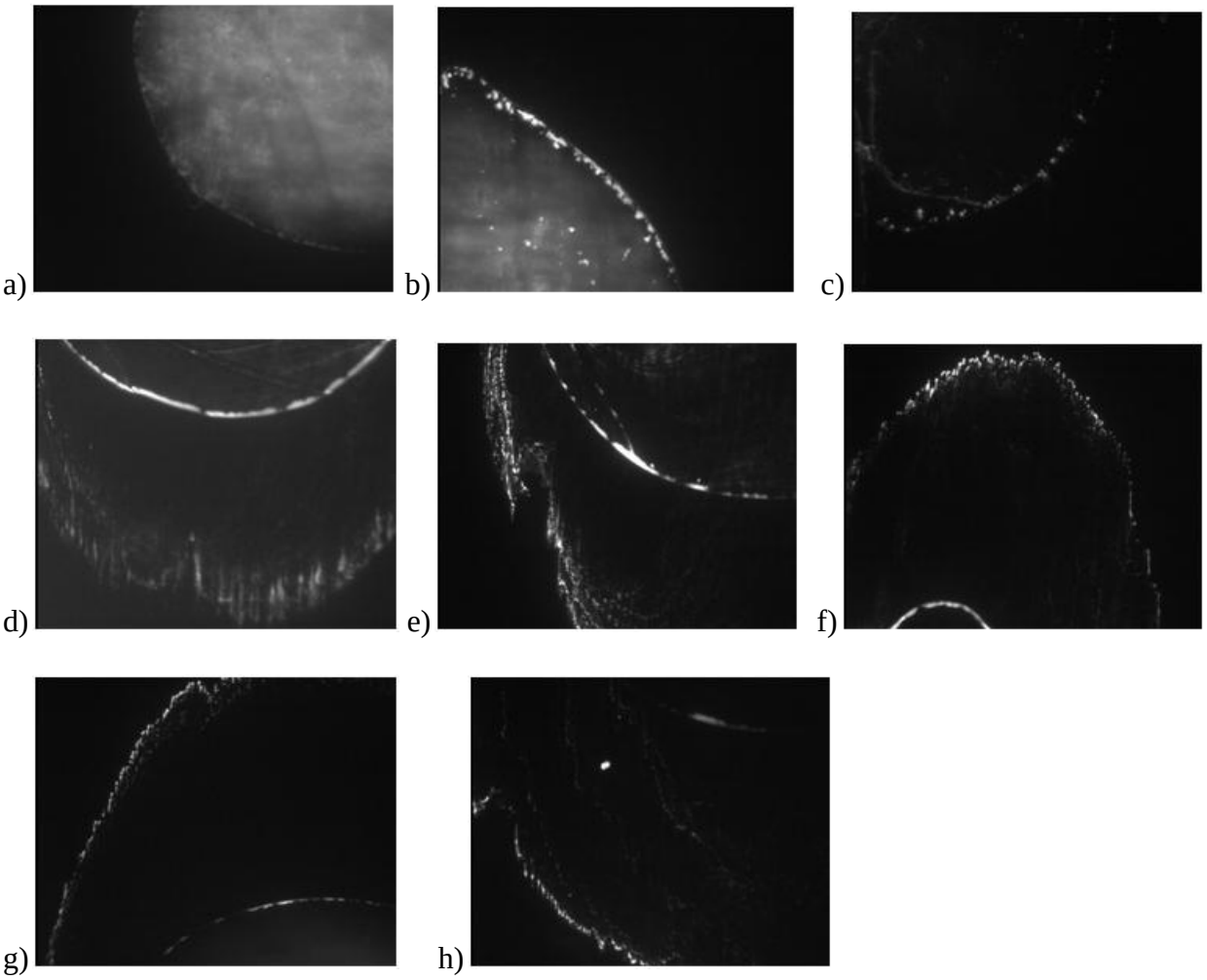

Figure 10. Spreading of drops of solution with different concentration of YOYO-1 and Lambda DNA in TBE solution YOYO-1: Lambda DNA: TBE (a) 2:0:1000 , (b) 1:13.4:1000, (c)

0.5:13.4:1000, (c) 0.25:13.4:1000, (c) 0.125:13.4:1000, (c) 0.063:13.4:1000, (c) 0.032:13.4:1000, (c) 0.016:13.4:1000

We choose a threshold to eliminate a background and calculated cumulative relative intensity for each picture and obtained a graph shows dependence of florescence versus YOYO-1 dye concentration for the same concentration of Lambda DNA. (Fig 11). The results show that maximum intensity of fluorescence in nanochannels was on Fig 10(e) which corresponds to 0.125 µl of YOYO-1, 13.4 µl of Lambda DNA dye and 1000 µl of TBE (4 times less than recommended). This optimal ratio was used for further experiments.

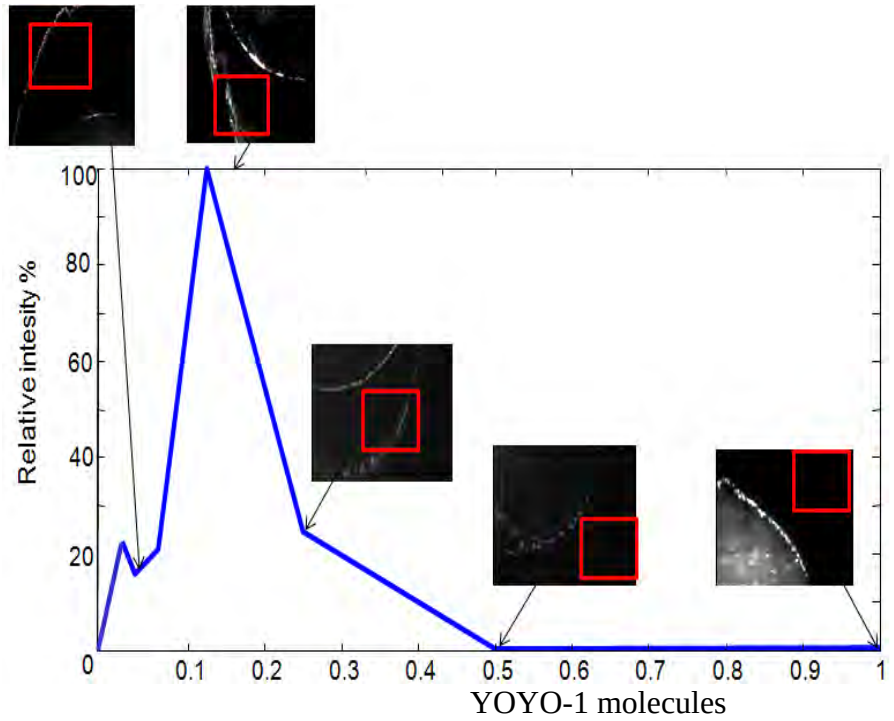

Figure 11. a) Dependence of relative fluorescent intensity versus concentration ratio YOYO-1 to 10 bp of DNA

5. Development of a two level chip with cross channels and porous layer as separation media.

Two layer chips which gave possibility not only to filter but also to collect separated molecules were fabricated. The second layer of a 500-nm wide nanochannels array perpendicular to the first was fabricated on the top silica nanochannels. The silica nanoparticle barrier was made in this layer for DNA accumulation. The second pair of wells was made in the opposite direction (Fig 12(a)). Then molecules from a drop moved through the top channels accumulated along the barrier and penetrated through the porous roof into the bottom layer and moved in perpendicular direction. The drops of a buffer solution made the chip wet (Fig 12(b)) provided conductivity.

Applied electric field to the wells can drive DNA in the top channels and provide fast accumulation at the barrier. Molecules that penetrate into the first layer can be removed from the channels by an electric field applied to the pair of wells in the bottom layer.

Another type of chip with two perpendicular layers and cross wells was fabricated with a macrochannel in the top layer to study possibilities of molecules penetration into the bottom layer during the movement in the top one with and without electric field application (Fig 12(c)). The crosscuts of the chip in different directions were made by SEM. The crosscut made perpendicular to the first layer is shown in Fig 13(a) and perpendicular to the second in Fig 13(b). The roof of the first layer can vary in thickness 200-500 nm to provide a difference in time of penetration for optimization the molecules separation. For better estimation of the thickness of the separation layer we made chips with parallel channels in two layers (Fig 14).

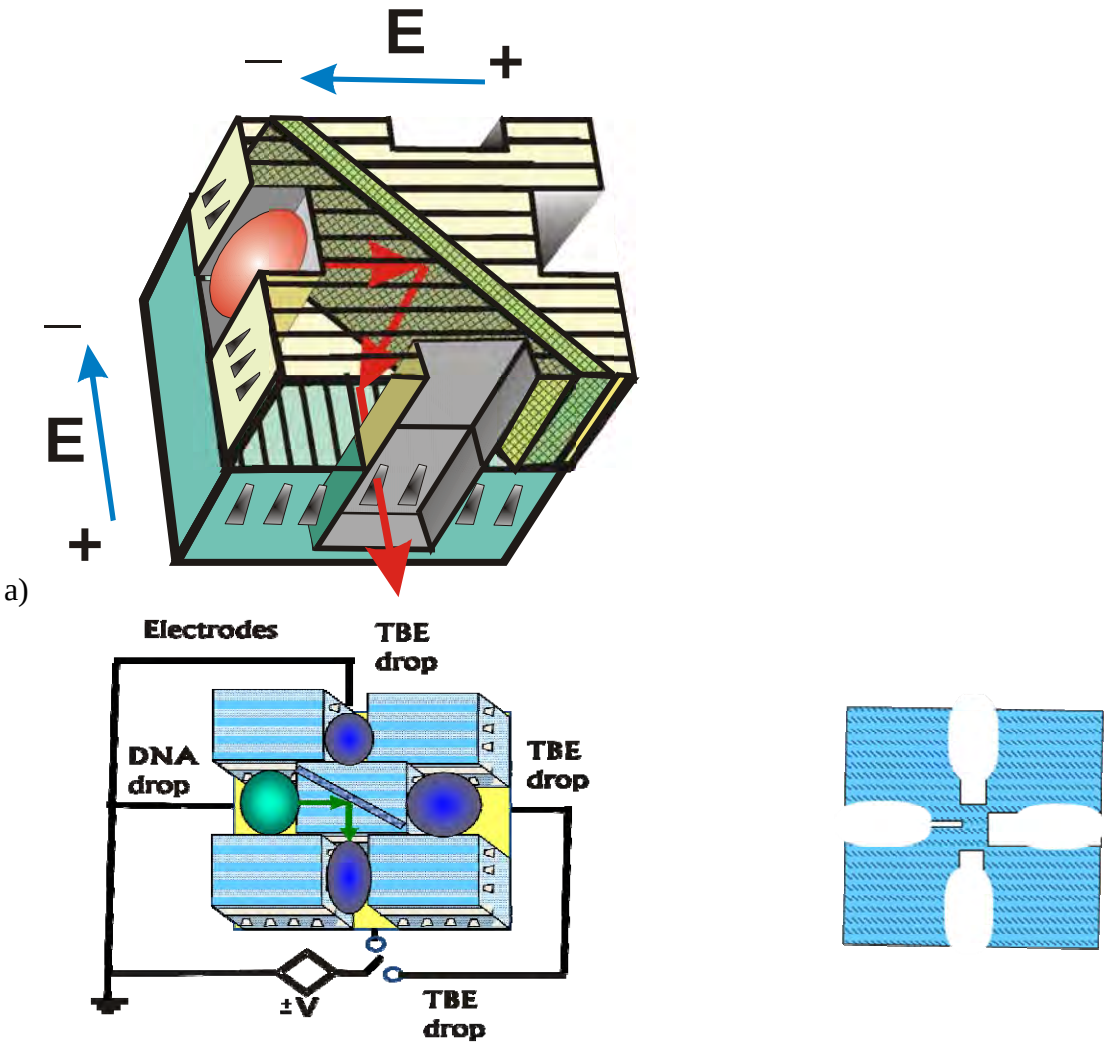

Figure 12. (a) Schematic of molecules penetration from the top to the bottom layer, (b) Sample with 2 layer nanochannels, barrier and application of electric field, c) Chip with macrochannel

Figure 13. a) crosscut along top channels, b) crosscut perpendicular top channels

Figure 14. Chips with different separation thickness of the roof

The result of the experiment with microchannel chip (Fig 12(b)) is shown in Fig 15. DNA moved in the second layer penetrated into the lower layer through the roof and is nicely seen in nanochannels in the perpendicular direction. However, the wetability of the chip surface and arbitrary penetration results in chaotic locations which creates difficulties in study speed of penetration of different types of DNA as well as their stretching with impact of the electric field.

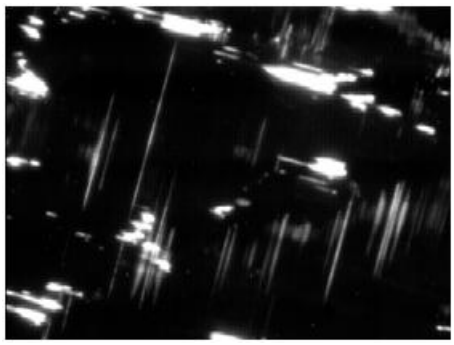

Figure 15. Fluorescence in the second layer.

6. Chips with barriers for separation

The next group of experiments was conducted using samples with channels and thin barrier from nanoparticles manufactured perpendicular to the channels. The barriers were fabricated by additional illumination of photoresist patterns after interferometric lithography on a mask aligner before silica particles spinning. A chip with a barrier (3 μm) is shown in Fig 16 (a), enlarged area of interest is shown in Fig 16 (b) from the top and in Fig 4 (c) from the side. It is also possible to make several barriers for different types of filtration. A chip with three barriers perpendicular to the channels is shown in Fig 16 (d), enlarged area of interest is shown in Fig 16 (e) from the top and in Fig 16 (f) from the side.

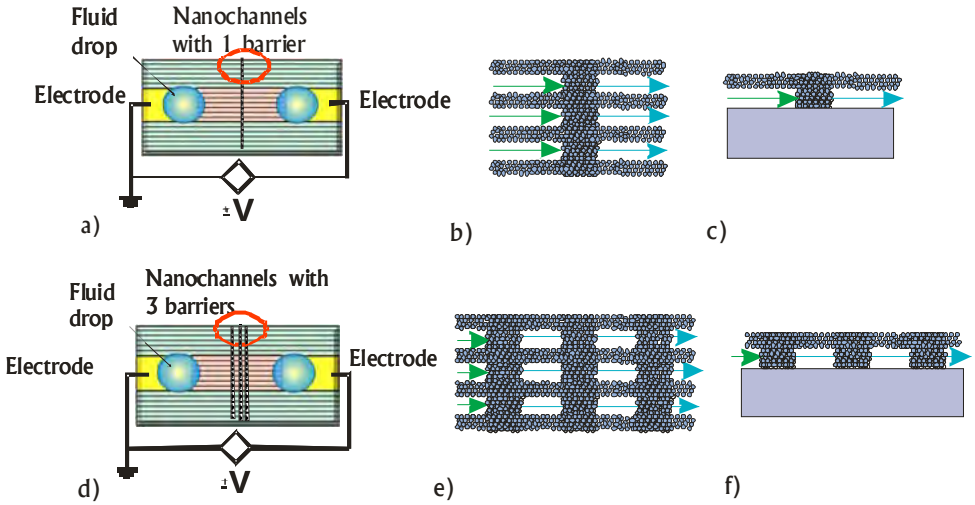

Figure 16. (a) Sample with nanochannels and 3 um barrier, (b) enlarged area of interest from the top and (c) from the bottom (d) with three 3 um barriers, (e) enlarged area of interest from the top, (f) from the bottom

Experiments conducted with DNA showed DNA movement into the channels and accumulate along the barrier (Fig 17 (a)). The buffer solution filled the well on the other side to provide the chip conductivity. Applied electric field increased DNA accumulation (Fig 17 (b)) and then DNA penetrated through the barrier (Fig 17 (c)). Accumulation on three barriers is shown in Fig 17 (d). In this case we observed DNA penetration over the roof through a drop (Fig. 17(e) taken with pump laser and Fig 17 (f) taken with regular white illumination). Opposite electric field moved DNA from the barrier as it is shown in Fig 18 (a). Fig 18 (b) is taken with pump laser and regular illumination allows us to see the barrier and the channels on the left. Drops of fluid were going over the barrier (Fig 19 (a)). They appeared and disappeared from the porous surface due to the applied electric field and capillarity effects (Fig 19 (b)). The electric field enlarged the drops especially on chips with several barriers (Fig 19 (c)).

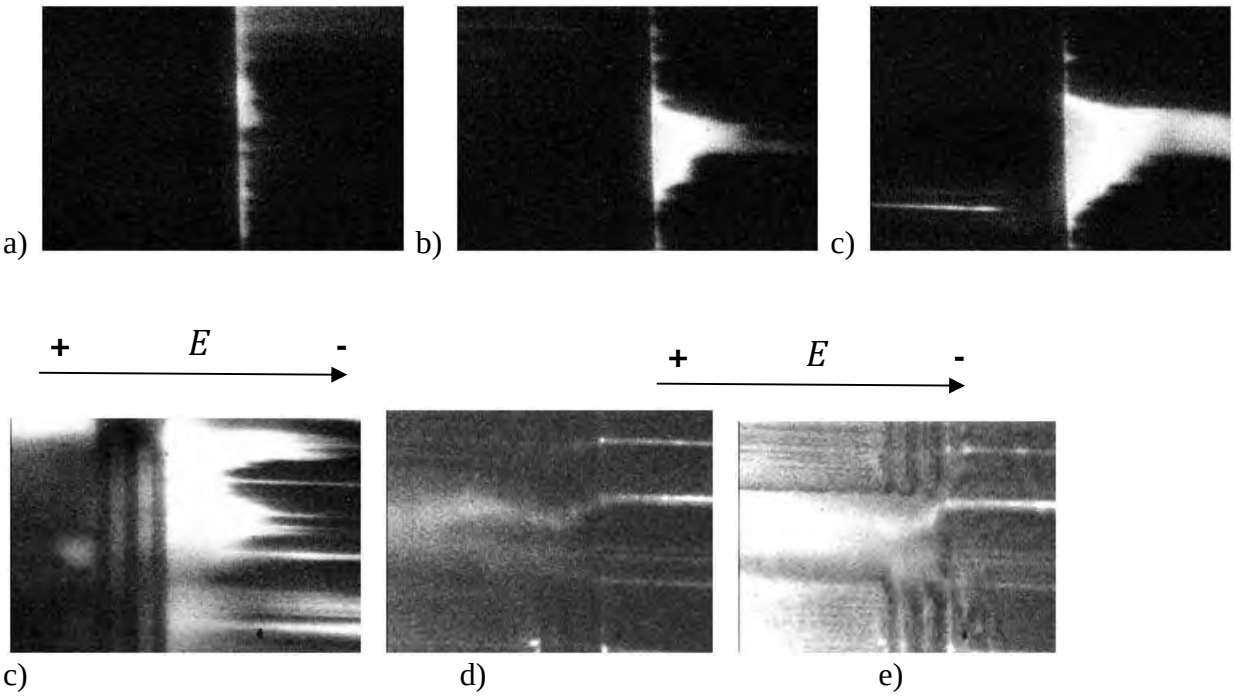

Figure 17. (a) DNA accumulation at the barrier, (b) DNA accumulation at the barrier with applied electric field, (c) DNA accumulation and penetration through the barrier, (d) DNA accumulation at three barriers, (e) DNA penetration through the drop on the surface over the barrier with electric field applied. The(picture was taken with laser pump and (f) and white illumination

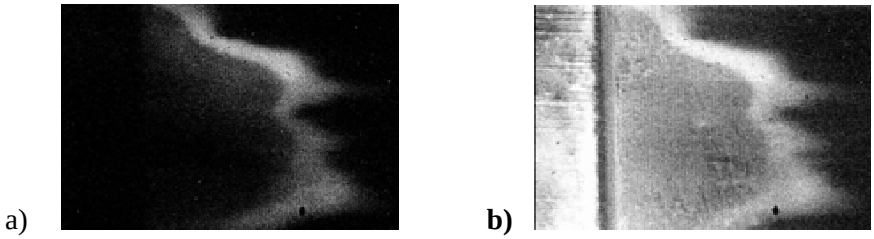

Figure 18. (a) DNA movement to the right side with electric field applied, (b) DNA movement to the right side with electric field applied (picture was taken with laser pump and white illumination).

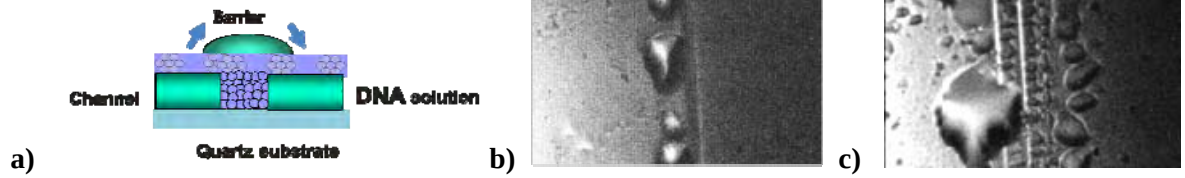

Figure 19. (a) Nanochannel chip with porous roof and liquid penetration through the roof over the barrier, (b) sample with nanochannels and one 3 μm barrier, (c) drops of fluid along three 3 μm the barriers with electric field applied (picture was taken with laser pump and white illumination)

The results of experiments showed that a waterproof cover on the roof is necessary to study the difference in DNA molecule penetration through the barriers as well as to study the influence of direct and pulse currents and temperature impact on the mobility. Chips with solid cover can have applications in separation of biological components, molecules and particles by size and mobility.

7. **Chips with bonded pyrex** roofs

The next approach was to use chips with channels etched in silicon wafer (oxidized to present a SiO_2 surface to the solution), covered by a solid Pyrex roof using anodic bonding (usual bonding conditions 1000 V and 350°C). The 25 μm wide by 1 μm deep channels were filled with nanoparticles were investigated for DNA separation by size. In an ideal case we need at least two barriers of nanoparticles under a solid roof for observing the separated DNA: one barrier for separation and the other for DNA accumulation, because we can observe fluorescent molecules only after they accumulate to a certain concentration (Fig 20).

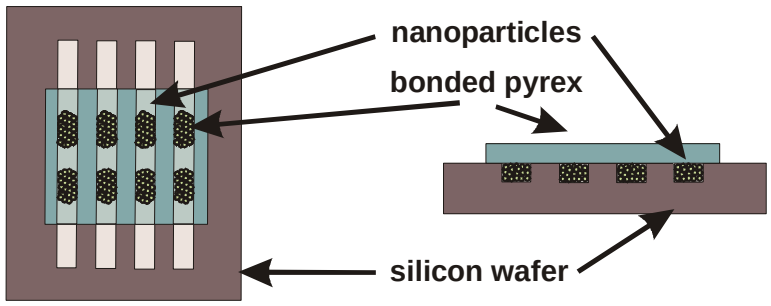

Figure 20. Channels etched in silicon with bonded pyrex and filled with nanoparticles.

We filled channels with nanoparticles from the wells to the side of the roof using electrophoresis. There is a great deal of flexibility in the channel and particle sizes we can use. A negative potential was applied to an aqueous solution of ~ 7 nm diameter nanoparticles on one side and positive to a drop of water on the other side. Nanoparticles were transported into the channels and filled them. Unfortunatly, the nanoparticle filling was not very uniform; to a large

extent, the nanoparticles accumulated on one or both edges of the pyrex (Fig. 21). Nevertheless, the experiments with this preliminary chip gave some promising results. In the experimental protocol, a negative potential was applied to DNA drop (positive to TBE drop on the opposite side of the ~ 5 mm wide roof). This arrangement provided DNA flow through the porous media consisting of dense arrays of 7 nm nanoparticles (2- to 3-nm pores between the nanoparticles). All of the following pictures are taken with the DNA drop on the top of the picture and TBE buffer solution on the bottom, so the flow is top to bottom. We used Lambda and LMW DNA solution with YOYO-1 dye and observed DNA accumulated at the edge of the porous media (Fic.22 (a,b)).

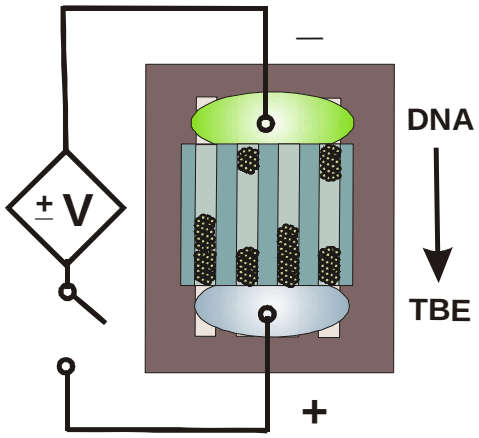

Figure 21. Chip with nanoparticles and applied voltage

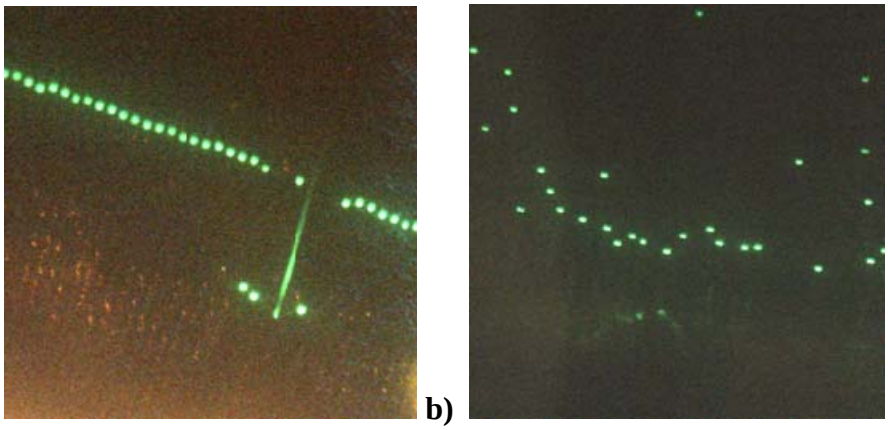

Figure 22. a,b) Lambda DNA dyed by YOYO-1 in nanochannels 488 nm wavelength illumination.

In experiments with Lambda DNA large conglomerations are nicely seen in channels with nanoparticles in white light together with laser illumination 488 nm (Fig.23). The DNA seems to be aggregating at sites within some, but not all, of the channels; this is probably related

to the nanoparticle filling non-uniformity. In a zoomed region of accumulation in a picture Fig.24 (a) taken in laser illumination we observe Lambda DNA large conglomerations blocking the channels (Fig.24 (b)). Then we conducted the same experiment with LMW DNA (200 bp) also dyed by YOYO-1. The molecules passed through the channels and mostly accumulated in small areas on the edges of channels were the pyrex was bonded (Fig.24 (c)). The zoomed region of accumulation Fig.24 (d) shows that concentration of stacked molecules in this case is much smaller probably because of higher mobility of smaller molecules through nanoparticle regions.

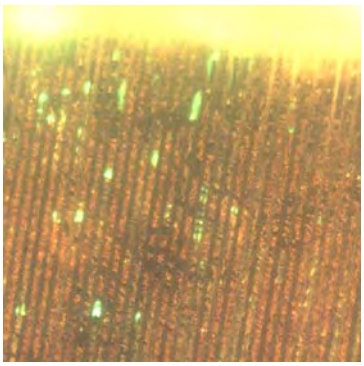

Figure 23. Lambda DNA dyed by YOYO-1 in nanochannels, 488 nm wavelength and white-light illumination.

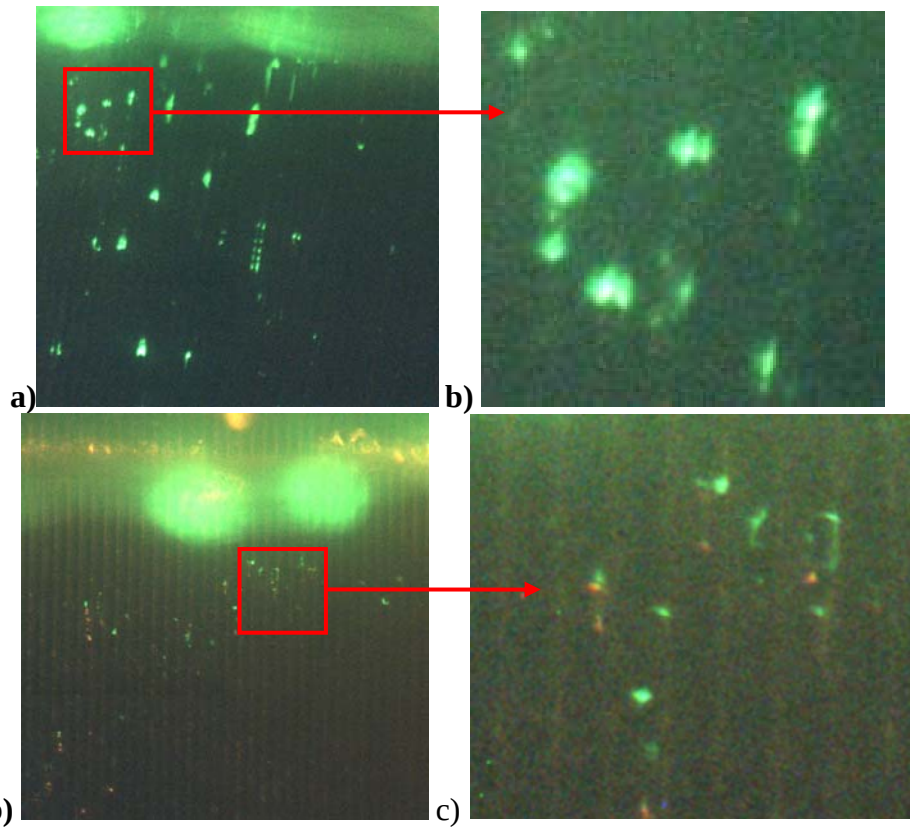

Figure 24. Lambda DNA dyed by YOYO-1 in nanochannels: a) 488 nm wavelength illumination, b) expanded view of region in red square, **c)** LMW DNA dyed by YOYO-1 in nanochannels, 488 nm wavelength and white light, b) expanded view of region in red square.

8. Separation of DNA mixture in chips with channels etched in silicon with bonded pyrex roof.

Taking into consideration the difference of penetration the following experiments were conducted with a mixture of Lambda DNA dyed by YOYO-1(excitation wavelength 488 nm; peak fluorescence wavelength 509 nm) and LMW dyed by Hoechst 33258 (excitation wavelength 365 nm and peak fluorescence wavelength 461 nm). The ratio was adjusted to the optimum ratio of dye to DNA determined in previous measurements. Additional pump laser and a chopper were added to our set up to switch pump illumination (Fig 25). The pictures (Fig 26 (a,b)) taken in 488 and 365 nm illumination show locations of blue and green fluorescence. The pictures were taken several times to confirm the temporal stability. The picture taken with 488 nm and white light illumination (Fig. 26(c)) indicates the location of the channels. The overlapped green and blue layers of Fig 26(a) and Fig 26(b) clearly show separation of blue and green fluorescence in the channels filled with nanoparticles (Fig.26(d)).

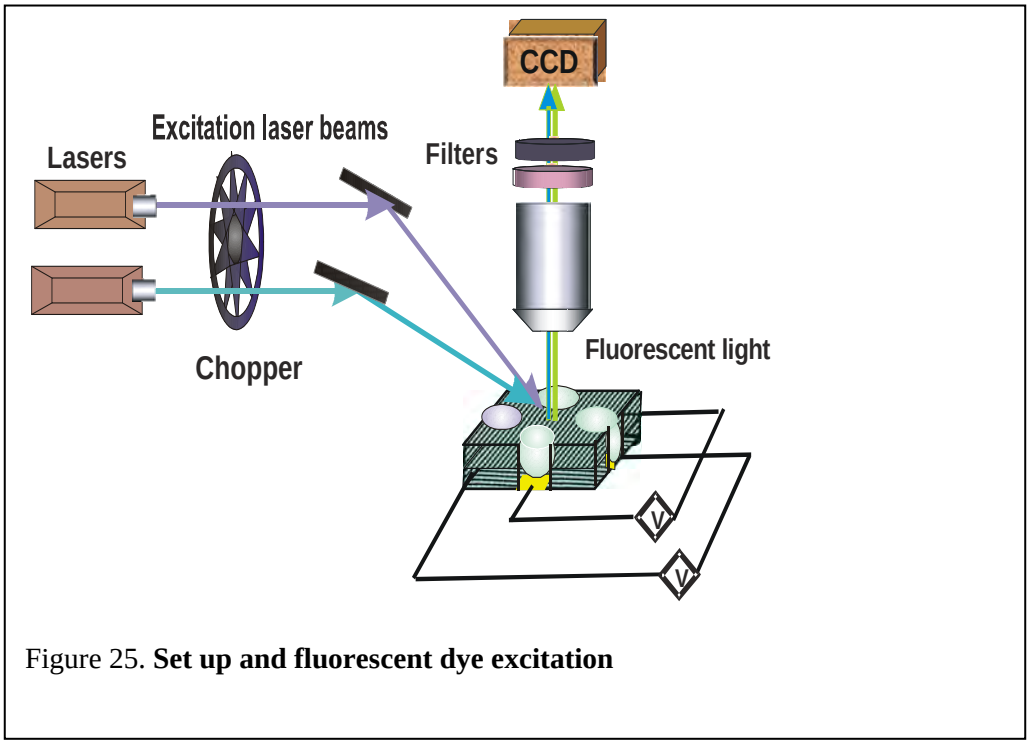

Figure 25. **Set up and fluorescent dye excitation**

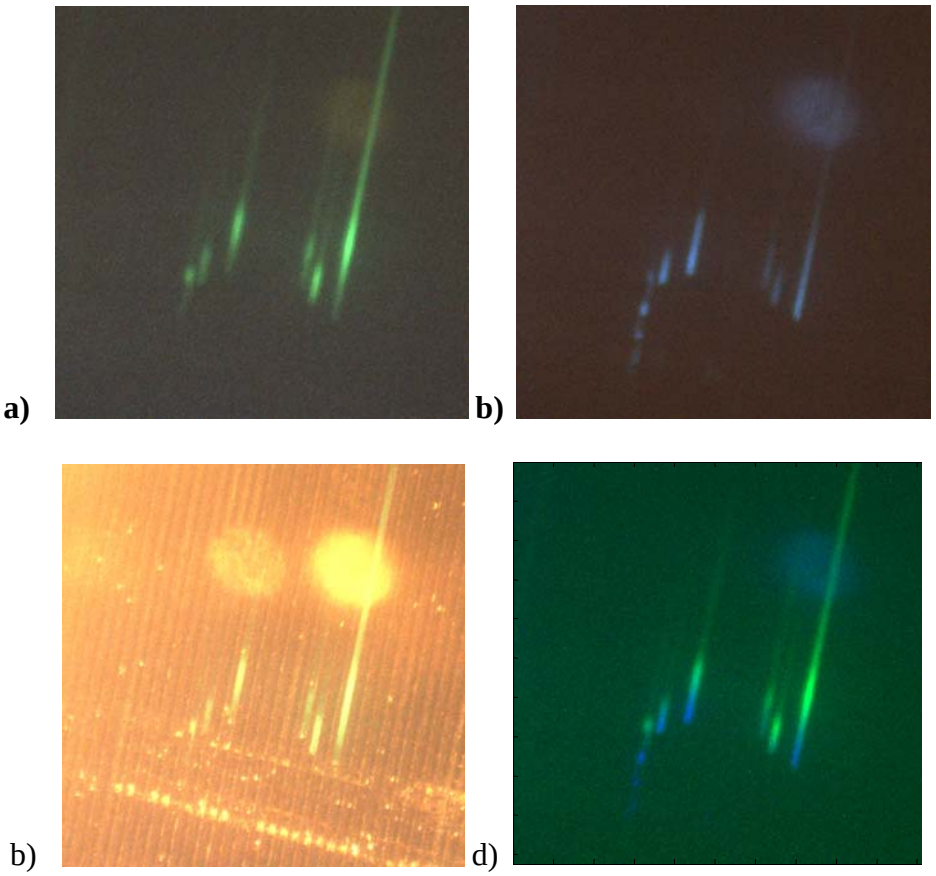

Figure 26. Mixture of Lambda DNA dyed by YOYO-1 and LMW dyed by Hoechst: **a)** 488 nm illumination; **b)** 365 nm illumination; c) white light illumination, d) sum of green and blue layers of figures (a) and (b). The line of scattering at the bottom is due to a scratch on the roof and is not indicative of DNA accumulation.

In order to confirm separation, the next experiments were made with opposite mixture of DNA with dye. Lambda DNA dyed by Hoechst and LMW dyed by YOYO-1. However, the blue fluorescence was in front again (Fig 27 (a,b)). Also in this experiment in the same overall regions, we observed some channels with only blue fluorescence and some with only green (Fig. 28(a,b)). In this case we can suggest that we have separation of dyed molecules due to size or quality of channels

a) 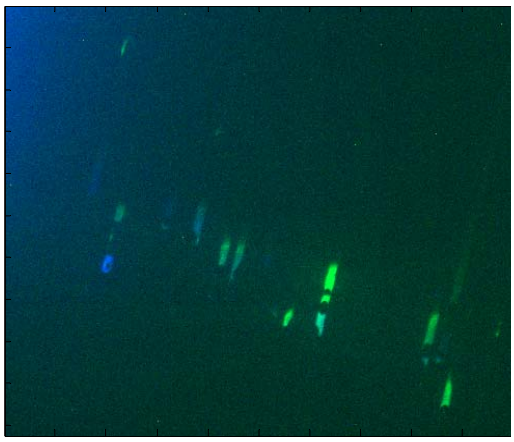 b) 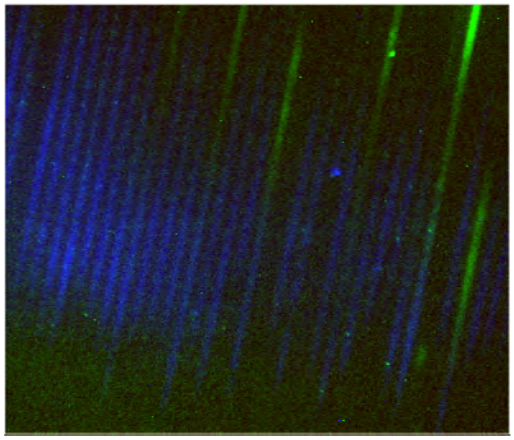

Figure 27. (a, b) Lambda DNA dyed by Hoechst and LMW dyed by YOYO-1, sum of green and blue layers of figures taken with 488 and 365

a) 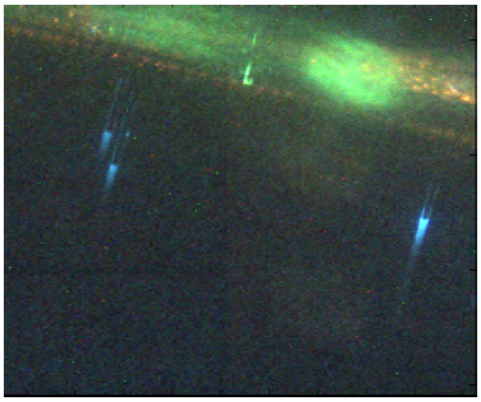 b) 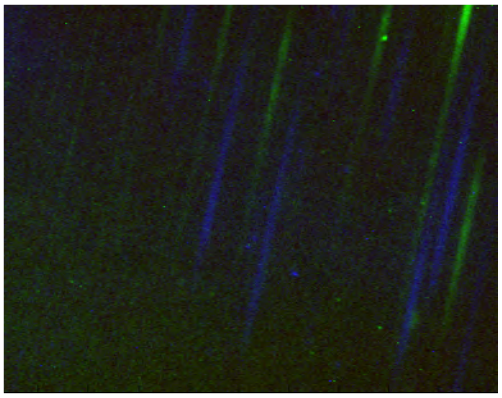

Figure 28. (a,b) Some channels with only blue fluorescence and some with only green, mixture of Lambda DNA dyed by Hoechst and LMW dyed by YOYO-1 , composite of pictures with 365 nm and 488 nm illumination.

In spite that the chips of this design gave good results in separation, there was defined localization of separated molecules for extraction due to non-uniformly filled macrochannels

(Fig.21). So we decided to return to our previous chip design. Due to the possibility of independent mobility of both the dye and the DNA molecules, it is difficult to determine if we have separated the dye molecules or the DNA molecules.

9. Fabrication and investigation of a chips with different cover using ALD deposition

We decided to solve the problem with DNA penetration over the roof of the barriers by sealing of the roof of our nanochannel chips and discovered that spin on glass or PDMS are hydrophobic and do not allow liquid penetration at all, all types of urethane prepolymers or nitrocellulose block channels completely. Molecular deposition (CVD) of SiO_2 or Si_3N_4 decreases DNA penetration through the roof and solution evaporation but does not prevent it completely. Only atomic depositions (ALD) made after CVD deposition almost completely prevents passing DNA through the roofs (Fig. 29). In case of ALD or CVD depositions we have to change technique of etching wells. Lithographical method when we put photoresist, used a mask for illumination, etched wells and washed out photoresist did not work well for chips because we could not remove photoresist out of channels completely due to the lack of pores in roofs. So we began to use just appropriate mask for etching.

.

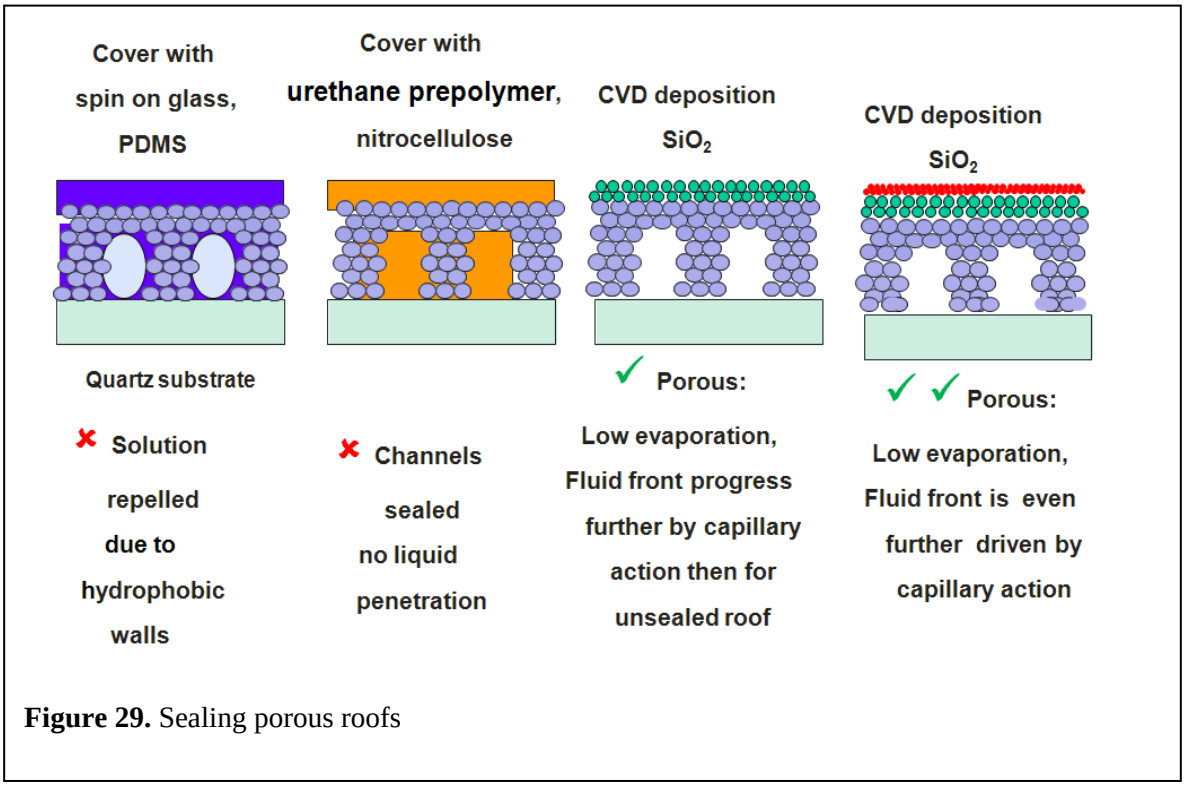

Figure 29. Sealing porous roofs

The initial design of chips had uniform barriers but disadvantages in rapid evaporation through the porous roof. Different kinds of depositions change evaporation over the chip roof. Evaporation can be estimated by the distance of liquid penetration through the channels. If we put a drop of liquid on the porous roof we can see that penetration of liquid through the channels is approximately 1.5- to 2-mm. The same penetration we observe if we put the drop into the well. (Fig.30 (a)). In this case DNA solution easily penetrates through roofs with ~ 15 nm pores,

especially under applied electric field across the barriers. Chemical vapor deposition (CVD) of an 80- to 120-nm film of Si_3N_4 or SiO_2 over the roof reduces the evaporation and provides liquid penetration up to 3- to 4-mm (Fig.30 (b)). A further application of 10- to 20-nm thick atomic layer deposition (ALD) of silica (SiO_2) or alumina (Al_2O_3) over the CVD deposition reduces the roof pore size further and provides liquid penetration up to 5-8 mm and almost prevents DNA penetration through the roofs (Fig.30 (c)).

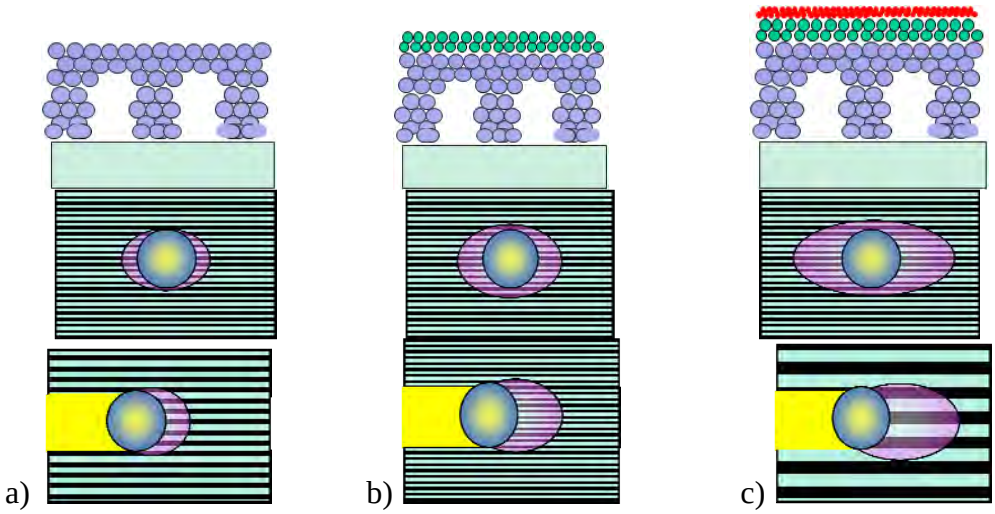

Figure 30. a) Nanochannel chip with porous roof and liquid penetration 1.5-2 mm , b**)** Nanochannel chip with porous roof and CVD deposition, liquid penetration 3-4 mm , c**)** Nanochannel chip with porous roof , CVD deposition and ALD deposition, liquid penetration 5-6 mm. The top figures show a schematic of the nanochannel structure; the middle gifures are the result of penetration from a drop of solution deposited on the roof; the bottom figues show the penetration into the channels for a drop applied to etched wells exposing the entrances to the nanochannels.

We investigated different types of atomic depositions. Ag deposition is not transparent for fluorescent light as well as for THz. Al_2O_3 deposition (note, that it requires different type of etching wells: BCl_3 instead of $SiHF_3$) is transparent, allows 5-6 mm of water penetration but prevents long distance DNA penetration through channels probably due to the positive charged walls. We applied an electric field (70 V/cm) to investigated chips and discovered that DNA did not penetrate more than 1-2 mm from the edge of well (Fig. 31). Changing the polarity of the potential caused only DNA oscillation in the area of penetration.

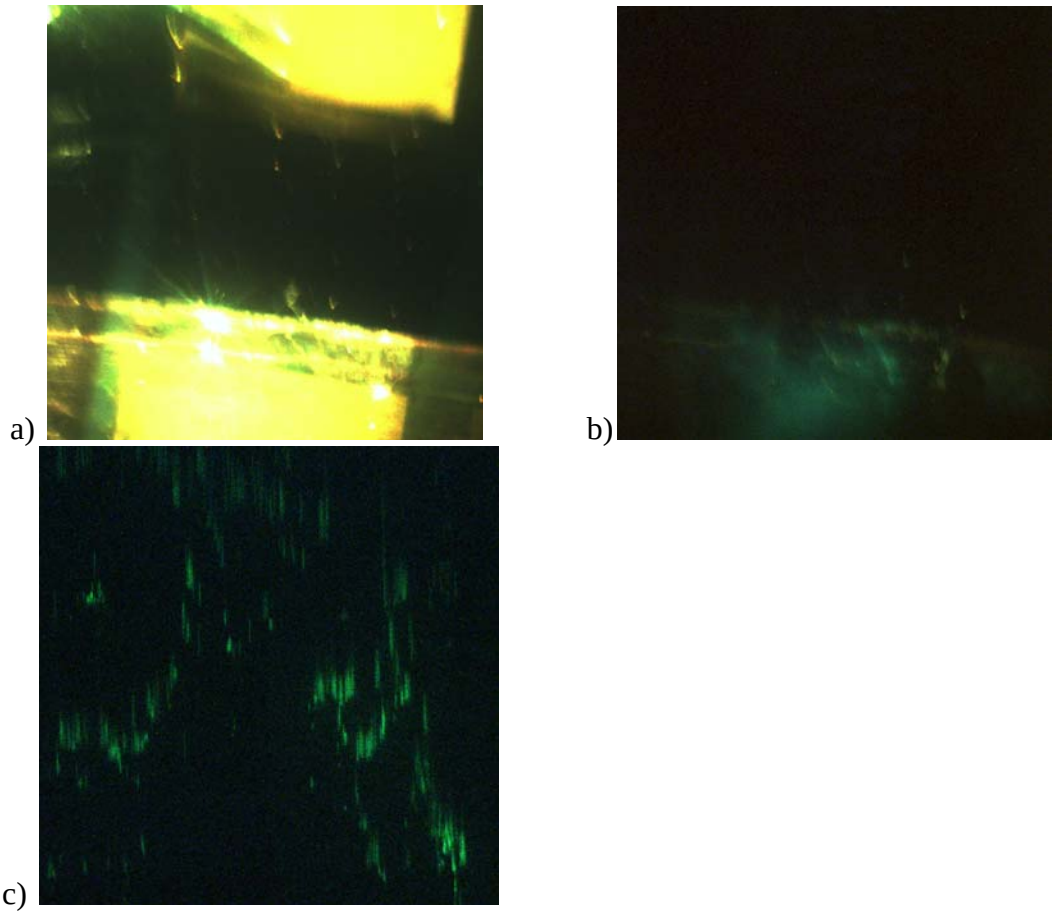

Figure 31. Al_2O_3 deposition, quartz chip with contacts, DNA solution on the bottom contact and TBE on the top a) white light 1-x magnification, b) 488 nm wavelength illumination, 1-x magnification, c) area near the bottom contact, 488 nm wavelength illumination, 20-x magnification

We found out that there was an influence of different ALD depositions on DNA penetration. SiO_2 deposition allowed 6-7 mm of water penetration and 2-2.5 mm of DNA penetration through the channels (Fig. 32). Applied electric field did not give good results because we could work only with silicon wafers with high conductivity. SiO_2 deposition on a quartz substrate requires special arrangements in a set up for ALD deposition which will be done in future.

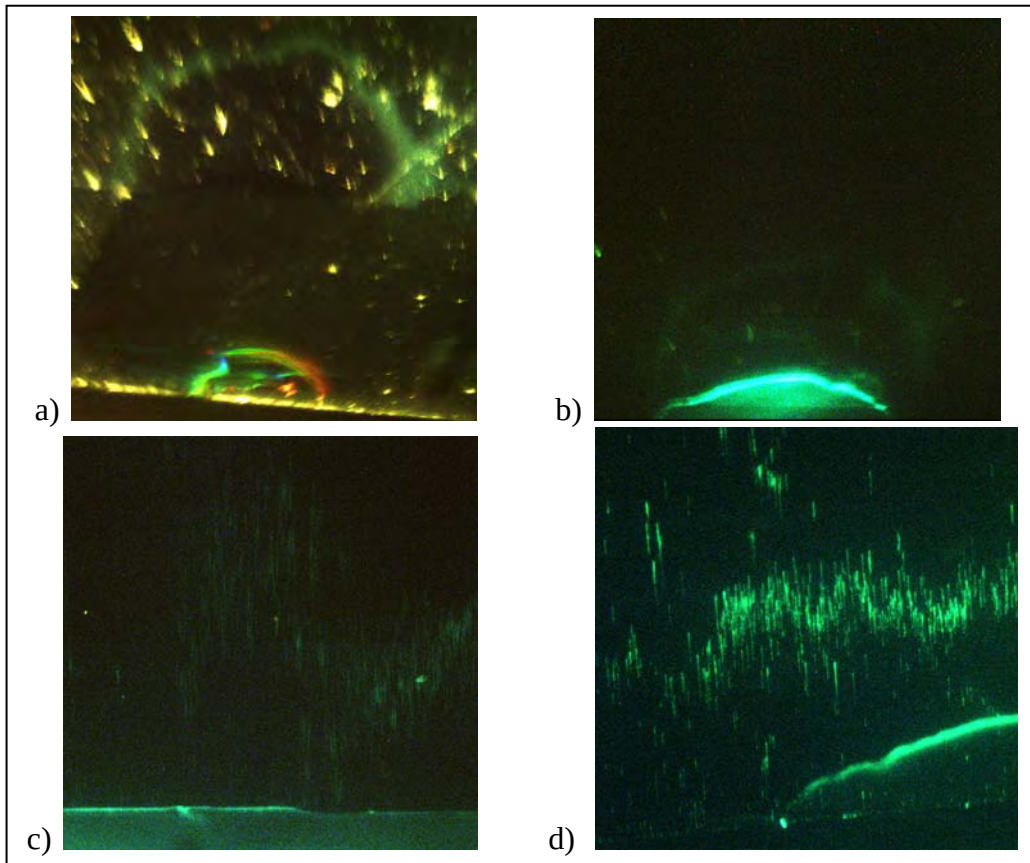

Figure 32. SiO_2 deposition , silicon chip with wells, DNA solution on the bottom a) white light 1-x magnification, b) 488 nm wavelength illumination 1-x magnification, c) area near the bottom well, 488 nm wavelength illumination 5-x magnification, d) area near the bottom well, 488 nm wavelength illumination 20-x magnification

We had 7-8 mm of liquid penetration in chips with HfO_2 deposition (combined picture is shown in Fig. 33(a)) and 2-3 mm penetration of DNA (Fig. 33(b,c)). We also conducted experiments with quartz chip with two barriers and HfO_2 ALD deposition (Fig. 34). DNA under influence of an electric field penetrated through channels and became stuck on the first barrier located 1 mm from the well. They could oscillate in this area when but did not pass through the barrier. We saw nothing on the second barrier. It appeared that the pores in the barrier also were covered with HfO_2 and did not allow DNA penetration at all. Probably we need cover the edges of the channels to prevent atoms penetration inside during deposition. So, we decided to make experiments only with CVD deposition.

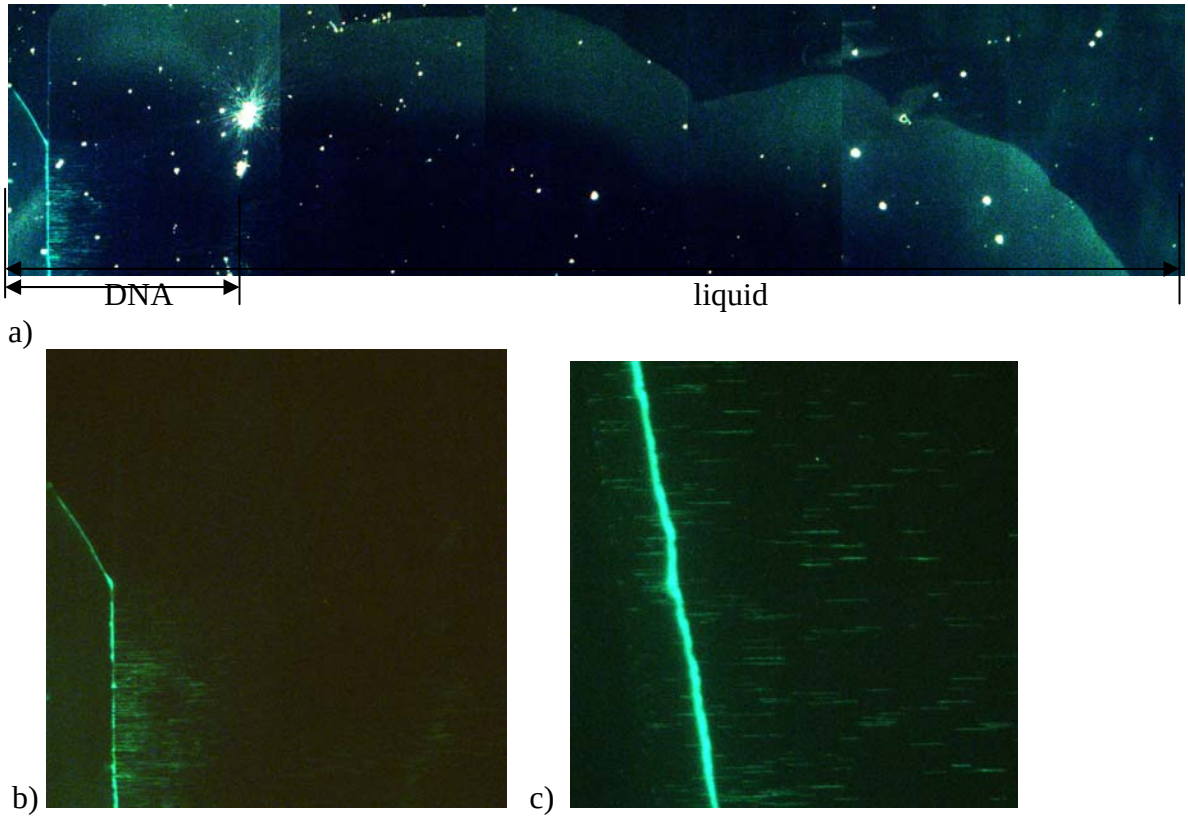

Figure 33. HfO_2 deposition, silicon chip with wells, DNA solution on the left a) white and 488 nm wavelength illumination 5-x magnification, c) area near the left well, 488 nm wavelength illumination 5-x magnification, d) area near the left well, 488 nm wavelength illumination 20-x

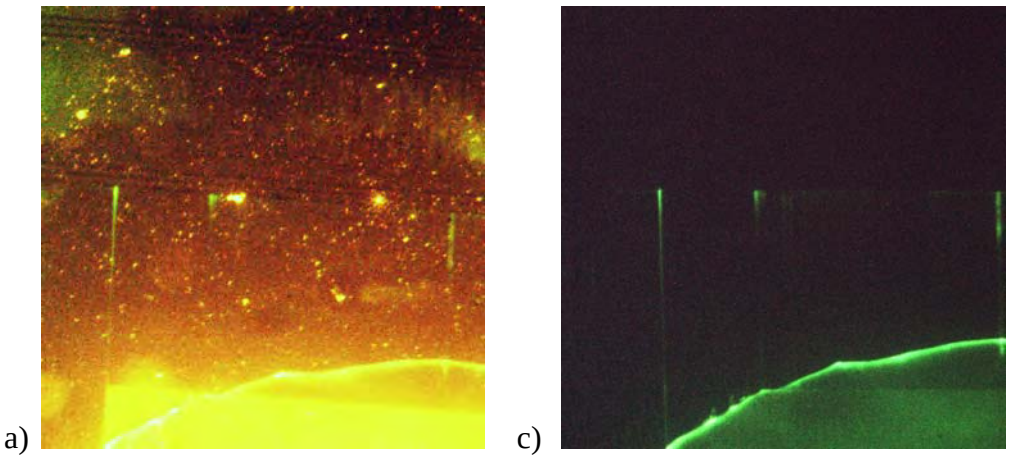

Figure 34. HfO_2 deposition, quartz chip with contacts and two barrier, DNA solution on the bottom contact and TBE on the top a) white and 488 nm wavelength illumination 5-x magnification, b) 488 nm wavelength illumination 5-x magnification

10. Investigation of penetration of DNA mixture in nanochannel chips with porous barriers using illumination of two lasers.

We investigated separation of DNA species using porous barriers in nanochannel We use a mixture of Lambda DNA - YOYO-1 dye, LMW DNA - POPO-3. Black and white cameras are more sensitive and can give us information about dyes localization if they are excited by different wavelength sources. Fig 35(a) shows the edge of a well (on the left, DNA flow to the right) three minutes after the mixture of Lambda (YOYO-1 dye) an LMW DNA (POPO-3 dye) was put into the well and both dyes were excited by 488 nm wavelength. Fig 35(b) is the same spot illuminated by 532 nm wavelength light which excited POPO-3 dye only and shows localization of LMW DNA molecules. The subtraction of Fig 35(b) from Fig 35(a) gives us the picture of λ-DNA localization labeled with YOYO-1 dye only (Fig 35(c)). Note that only the λ-DNA is observed in the nanochannel region.

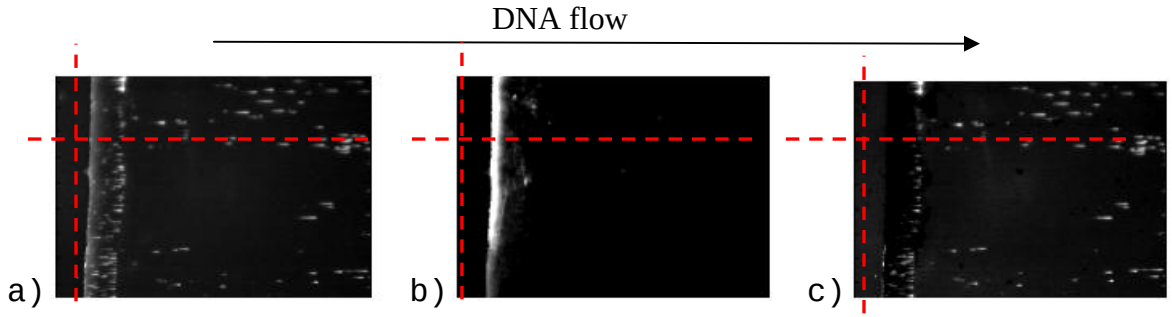

Figure 35. (a) fluorescence of λ- (YOYO-1) and LMW- (POPO-3) DNA exited by 488 nm ,
(b) fluorescence of LMW (POPO-3) DNA excited by 532 nm ,
(c) subtraction of the pictures – localization of λ-DNA.

The crosscuts of the pictures show us localization of λ- and LMW-DNA – blue line, LMW-green line, only λ DNA –red line in horizontal and vertical directions in Fig. 36 (red dashed lines). We see that the LMW DNA is more concentrated just at the edge of the well while the λ-DNA with YOYO-1 is distributed inside the nanochannels. The crosscuts also give us also information on the concentrations of DNA Fig. 36 (a, b).

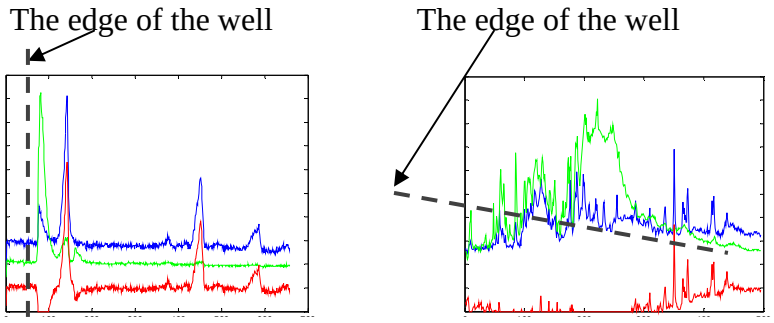

Figure 36. fluorescence of Lambda (YOYO-1) and LMW (POPO-3) DNA excited by 488 nmt – blue, fluorescence of LMW (POPO-3) DNA excited by 532 nm – green, subtraction of the pictures – localization of Lambda DNA -red.

The same mixture of λ- and LMW-DNA, dyed with different dyes as above, was dropped in one well (right) and a buffer solution in the other (left). Porous barriers for DNA separation was used (Fig 37 (a)) for separation experiments. When the electric field was applied the solution accumulated on the right side of the barrier and then after some delay appeared on the left. This is seen at 488 nm excitation (Fig 37(b)). However, the 532 nm excitation shows fluorescence only on one side of the barrier (Fig 37(c)). The crosscuts of the pictures (blue and green) and the difference between the pictures (red) along the brightest channels are shown in (Fig 37(d)).

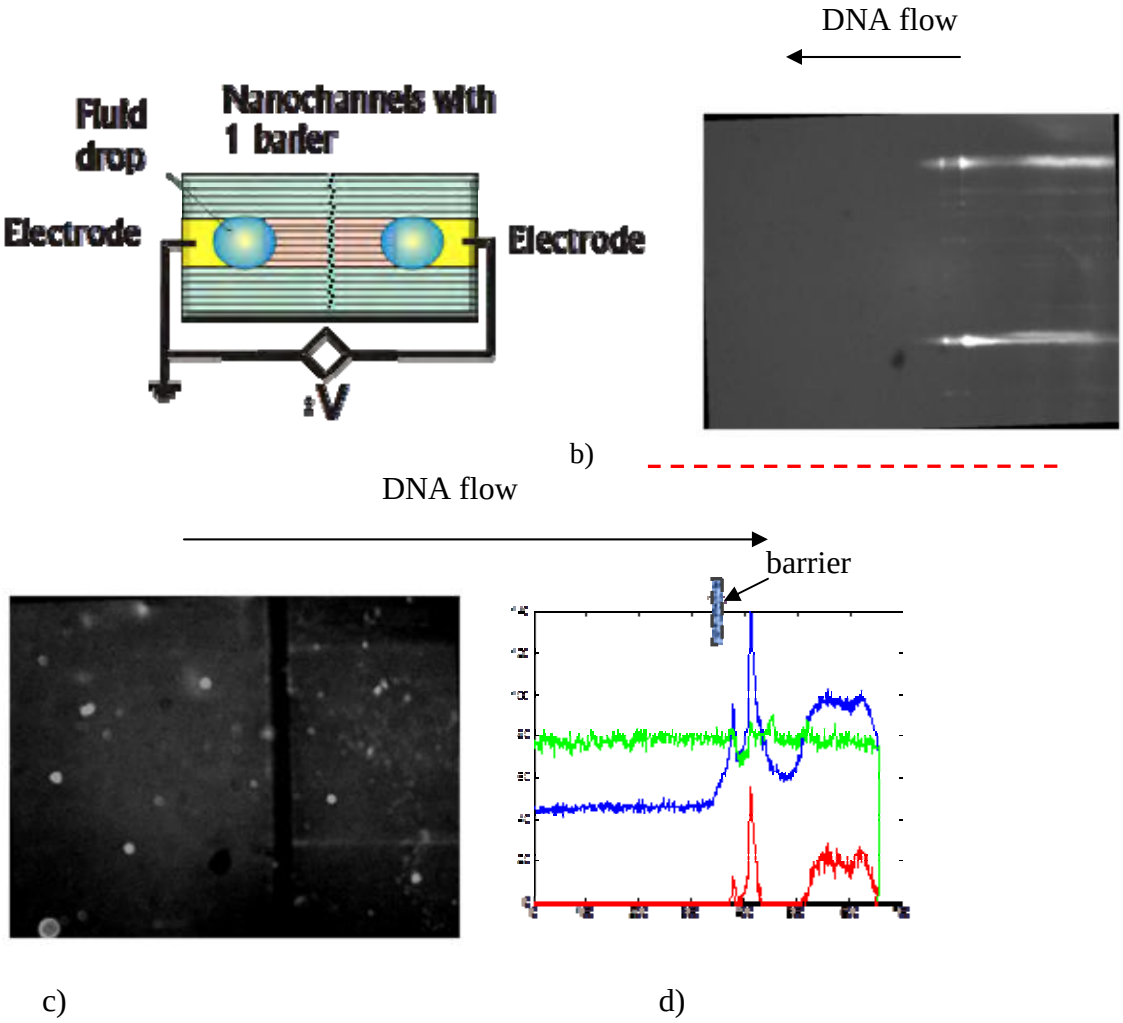

Figure 37. (a) Sample with nanochannels and 3 μm barrier,
(b) fluorescence of Lambda (YOYO-1) and LMW (POPO-3) DNA excited by 488 nm
(c) fluorescence of LMW (POPO-3) DNA exited by 532 nm light ,

We investigated separation of DNA species using porous barriers in nanochannel chips with CVD deposition using color camera. We use a mixture of Lambda DNA - POPO-3 dye, LMW DNA - YOYO-1 dye and mixture of opposite bonded components . In both cases we observed concentration of red fluorescence (POPO-3 dye) on the barriers (Fig.38). In these cases, barriers probably prevented penetration of molecules with POPO-3 dye. We observed green

fluorescence in several group of channels before the barriers. We think that separation of DNA by length took place in the nanochannels with barriers, but independent transport of dyes makes interpretation difficult.

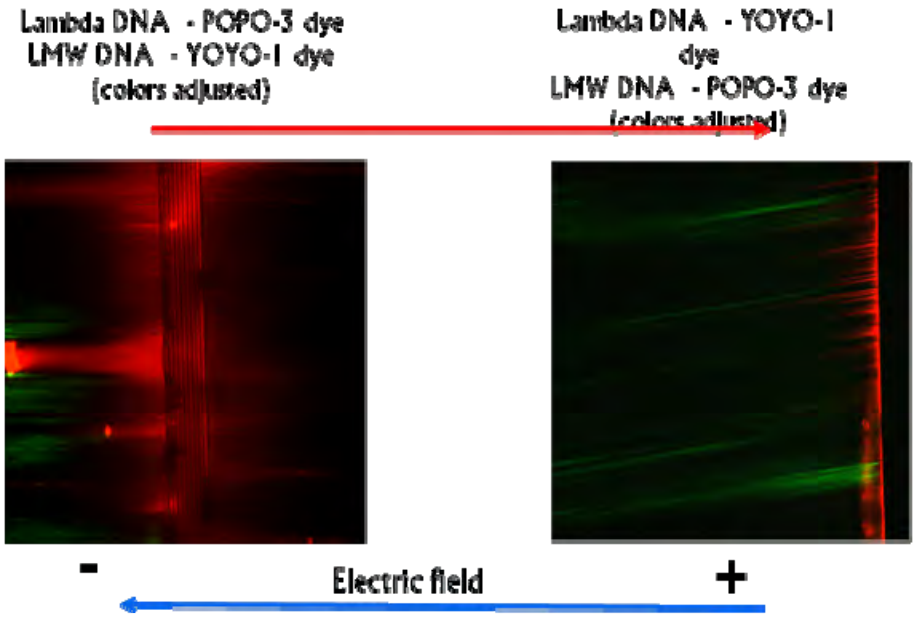

Figure 38. Separation of DNA species with different dyes using porous barriers in nanochannels

Another experiment was conducted with Lambda DNA dyed by SYTO 59 and LMW DNA dyed by YOYO-1. We used 488 nm and 636 nm pump illumination . Fig 39(a) shows that DNA dyed with YOYO-1 goes faster and passes through the barrier. If we use YOYO-1 dye for Lambda DNA and SYTO 59 for LMW DNA again we see that DNA with YOYO-1 dye moves faster (Fig 39(b)), reaches the barrier and starts penetrate (Fig 39(c)).

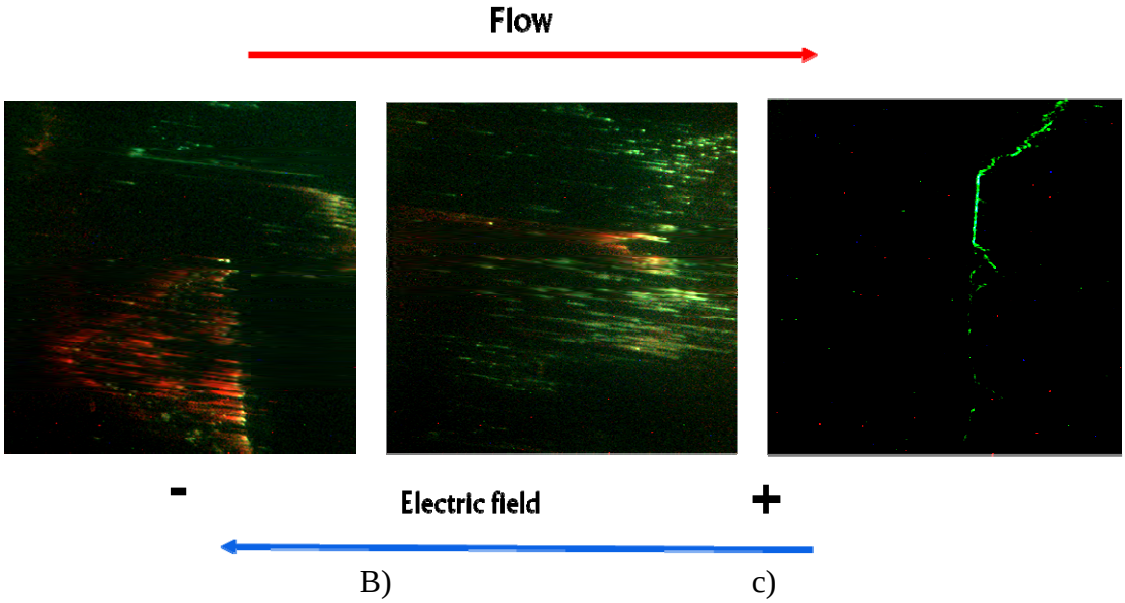

Figure 39. a) Lambda DNA dyed by SYTO 59 and LMW DNA dyed by YOYO-1 on the barrier, b) movement of Lambda DNA dyed by YOYO-1 and LMW DNA dyed by SYTO 59, c) Lambda DNA dyed by YOYO-1 and LMW DNA dyed by SYTO 59 on the

10. Experiments with drop of DNA mixture penetration through porous roof

Another set of experiments were conducted with drops of a mixture of different sizes of DNA bonded with different dyes put on the top of porous roofs over nanochannels. In this case the roof works as the separation media and we observed that molecules with certain dyes have different lengths of penetration. If Lambda DNA dyed by Hoechst and LMW dyed by YOYO-1 or in opposite combination**,** blue fluorescence of molecules with Hoechst was always in front of DNA dyed with YOYO-1 (Fig 40(a,b)).

a) 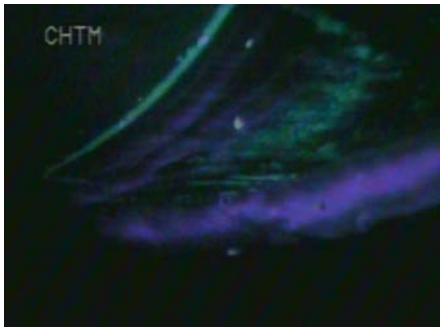

b) 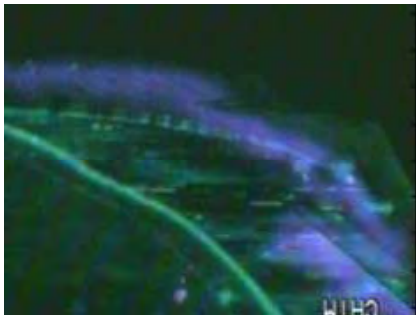

Figure 40. a) Mixture of Lambda DNA dyed by Hoechst and LMW dyed by YOYO-1**, b)** Mixture of LMW DNA dyed by Hoechst and Lambda dyed by YOYO-1

A drop of the mixture of Lambda and LMW DNA dyed by YOYO-1 and POPO-3 was put on porous roof and green fluorescent of YOYO-1 was seen ahead of orange. Interchange of dyes and DNA again resulted in green fluorescence in front of orange (Fig 41 (a,b)). Similar results were obtained from experiments with mixture of Lambda and LMW DNA with YOYO-1 and Syto 59 dyes (Fig 41(c, d)). So, in diffusion experiment DNA with certain dyes moves faster independently of length. Probably due to the non-covalent bonding, dye can separate from DNA, move independently and re-label another DNA strand (similar effect has been observed by other scientists with tagged antibodies).

.

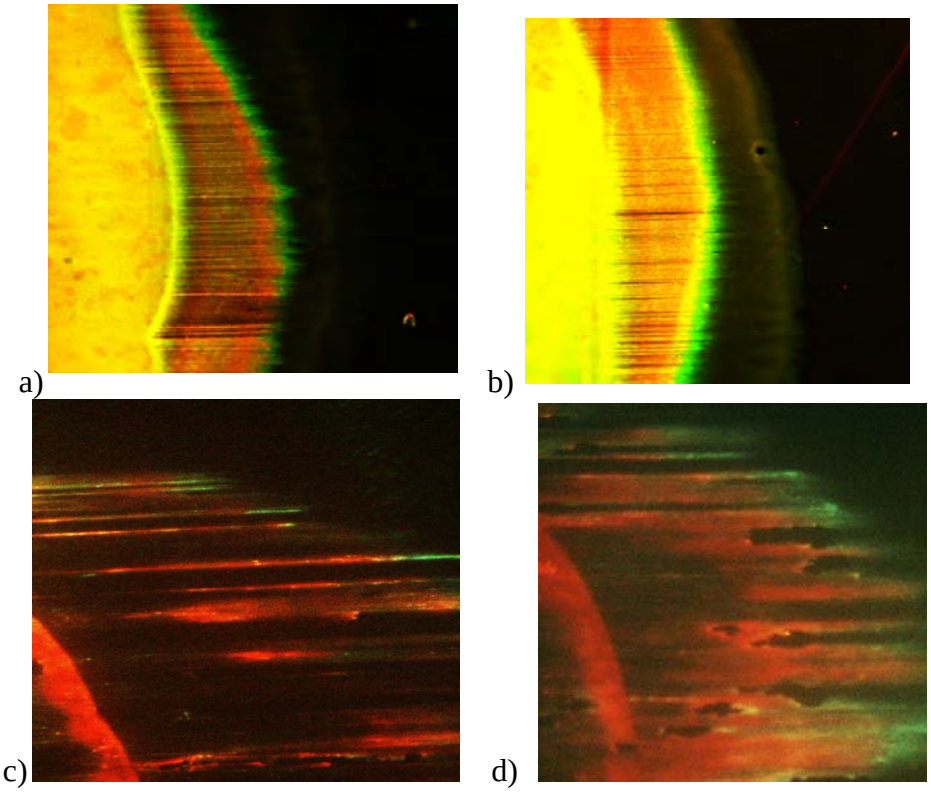

Figure 41 a) Lambda DNA - YOYO-1 dye, LMW DNA - POPO-3 dye , b) Lambda DNA - POPO-3 dye LMW DNA - YOYO-1 dye, C) Lambda DNA - YOYO-1 dye, LMW DNA - SYTO 59 dye, d) Lambda DNA - SYTO 59 dye, LMW DNA - YOYO-1 dye

These results are in a good agreement with SwatiGoyal results obtained on antibodies diffusion through 200 nm diameter nanochannel membranes. He showed that diffusion flux of goat anti-mouse IgG1 tagged with Alexa 546 antibody (red) is significantly higher than with Alexa 488 (Fig.42) [15]. We also have separate dyes migration caused by not covalent bonding.

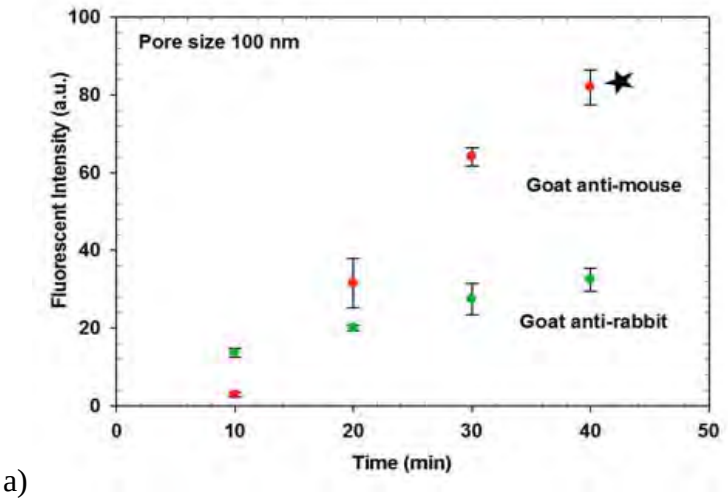

a)

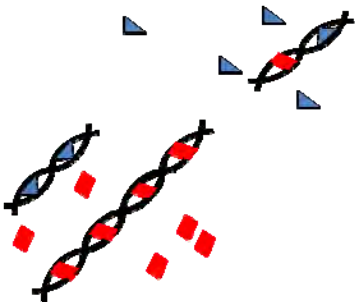

b)

Figure 42. Diffusion of antibodies through membranes, IgG1 tagged with Alexa 546 antibody (red) is significantly higher than with Alexa 488, b) Effect of Fluorescent Tags , problem with not covalent bonding: dye exchange

Penetration of mixture of DNA with different size bonded to different dyes through the CVD cover continues longer time but gives the same results as through porous roofs without cover. DNA dyed by Hoechst independently of size passes the roof faster and are nicely seen in front of DNA dyed by YOYO-1 in channels. DNA dyed by SYTO-59 or POPO-3 appears in channels later than DNA dyed by YOYO-1. In order to get rid of dye influence on DNA penetration probably we need to conduct experiments without dye and to check ratio of molecules before and after the experiment using gel separator or bio-analyzer.

11. Development of a device for DNA extraction from gel.

Gel media are well established for DNA separation. We have initiated a collaboration with Research Professor Anton Bryantsev in the UNM biology department. The main problem he identified was DNA extraction from the gel which is possible to do only with overwhelming losses (up to 75%) of the DNA (and is done quite crudely by cutting up the gel and separating the DNA from the components of the gel. The experiment we tried was to use our nanochannel chip with porous roof for DNA extraction from gels where DNA separation and banding has already been accomplished. A piece of gel with a DNA ladder was prepared. The gel was put on the top of our chip with porous roof and was held in place with a silicon wafer which also served as a top electrophoresis contact. A well etched for DNA accumulation was filled with TBE solution. An electric field was applied to the top Si wafer and to the electrode in the well (Fig.43). DNA moved from the gel into the channels through the roof and then along the channels to the well. Accumulation of DNA in the well was detected by fluorescence after adding YOYO-1 dye. This preliminary experiment showed the possibility of DNA extraction from gels and gives opportunities for future work on DNA separation and extraction. These chips with porous roof for DNA extraction from gels where separation have already taken place requires additional

barrier separating gel from a well. We hope that cover plate over the metal deposition around the wells will be used as the required barrier and will prevent mixture of DNA before collection

Further development of this technique will allow us to collect separated DNA from thin layers of gel (microns in thickness instead of millimeters) which can help to separate, indentify, and collect DNA in picoliter volumes for further analysis. There are many realistic applications for this capability in forensics and medical diagnosis.

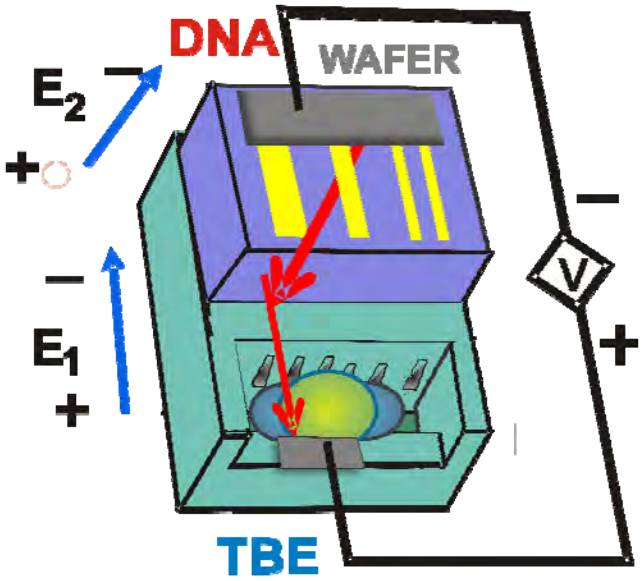

Figure 43. Use gel for separation DNA molecules and then nanochannel chip for filtration and extraction**.**

12. Design of a cover plate over wells area.

Experiments with DNA require large volumes of DNA solution (not less than 300 ng) especially if we are going to conduct experiments without dye and to check ratio of molecules before and after the experiment using gel separator or bio-analyzer. In order to increase the volume we need deeper wells. Additional deposition resulted in roof cracking. So we designed a cover plate from plastic or PDMS over the wells. This cover also can be useful in future design of an interface for pumping system in the wells. The problem was to glue the cover plate without blocking the channels. So; we decided to try additional metal deposition around the wells to prevent glue penetration (Fig.44). This chip will allow to install pumps over the wells.

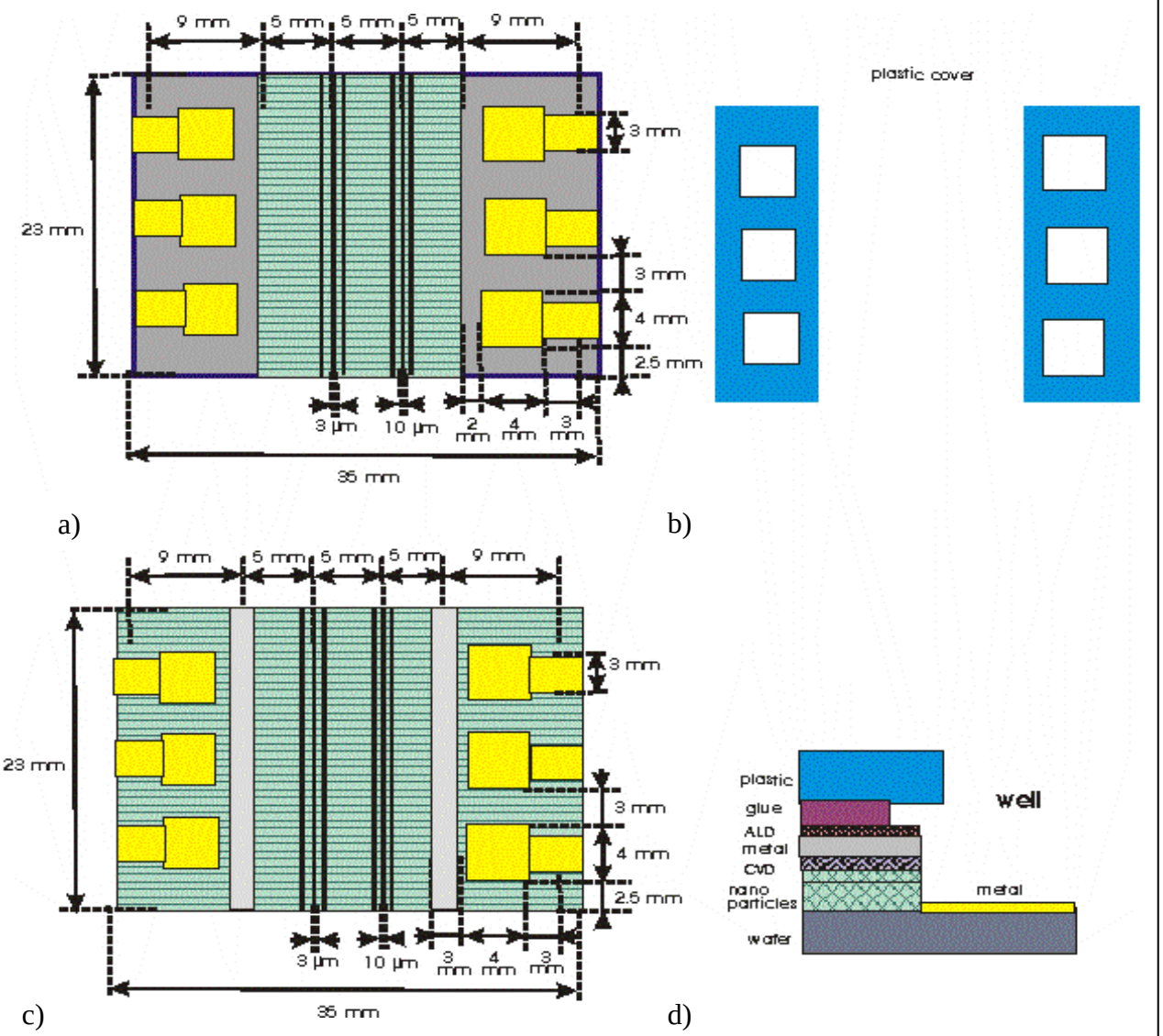

Figure 44. a) Nanochannel chip with barrier and metal deposition around wells, b) plastic cover, c) Nanochannel chip with barrier and stripes of metal deposition in front of wells, d) crosscut of depositions and cover plate near wells.

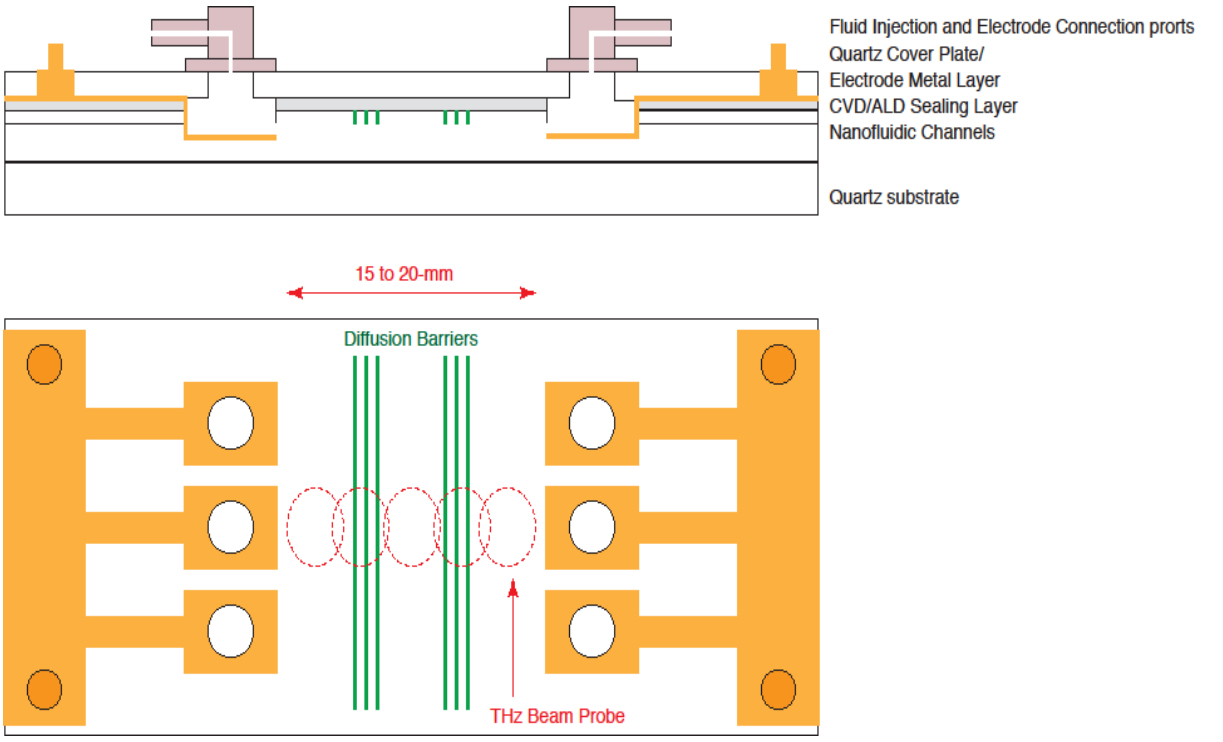

Figure 45. Chip for THz experiments and DNA separation

13.2. Development of a device for DNA extraction from gel

1. We are going to continue to work on the gel and nanochannel chip combination. In order to extract DNA of particular lengths separately we need a chip with a number of wells for accumulation of DNA of different sizes. At first the separation takes place in gel which is already in a contact with the nanoparticle roof. Then we can extract different sizes of DNA from gel into different collections wells (Fig.46). These chips can be very useful for rapid and efficient DNA separation and extractions.
2.

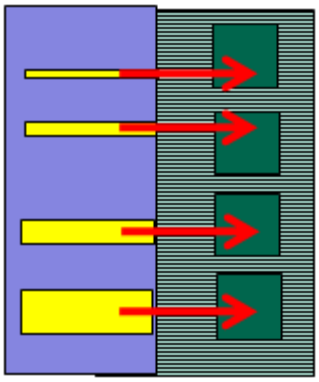

Figure 46. Use gel with nanochannel chip for separation DNA molecules, filtration and extraction**.**

13.3 Introduce spatially localized enzyme to observe dynamics of DNA fractionization (Fig.42).

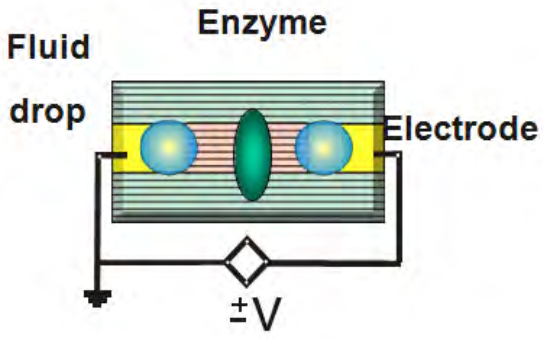

Figure 42. Chips for enzyme application to DNA

13.4 Use nanochannel chip covered with proteins penetrated from upper channels for DNA separation due to protein bonding (Fig.43).

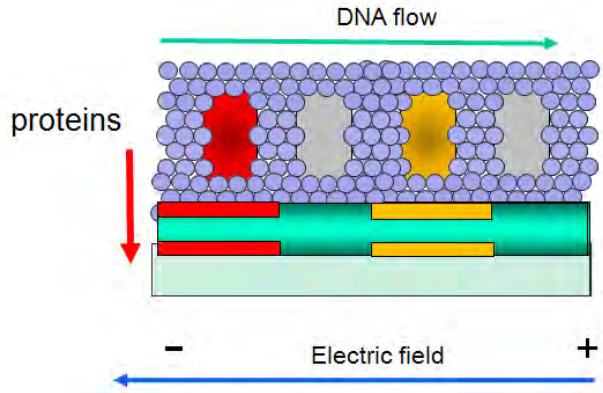

Figure 43. Chip for using protein for separation

13.5 **Detailed measurement of DNA stretching by labeling ends with different dyes and/or Q-dots (**Fig.44).

Figure 44. DNA with attached Q-dots

13.6 Study the influence of DC and pulse alternating fields as well as temperature impact on the mobility of different DNA molecules

13.7 THz Spectroscopy Measurements

We have continued to interact with Professor Elliott Brown (UCSB) and Dr. Edgar Mendoza (Redondo Optics) on the application of these nanochannels to THz spectroscopy of DNA and RNA samples. Our primary role is to supply the nanochannel samples. Over the course of this project several redesigns of the nanochannel geometry and materials have been carried out to improve the THz measurements. A preprint is attached with the major results of this work.

REFERENCES

1. Mark A. Burns, Brian N. Johnson, Sundaresh N. Brahmasandra, Kalyan Handique, James R. Webster, Madhavi Krishnan, Timothy S. Sammarco, Piu M. Man, Darren Jones, Dylan Heldsinger, Carlos H. Mastrangelo, David T. Burke,**"**An Integrated Nanoliter DNA Analysis Device **, "** *Science* 16 October 1998, Vol. 282. no. 5388, pp. 484 - 487 DOI: 10.1126/science.282.5388.484

2. *Harrison, D. J.*; *Fluri,* K.; Seiler, K.; Fan, Z. H.; Effenhauser, C. S.; Manz, A. Science 1993, 261, 895-897.

3. Cao, H.; Yu, Z.; Wang, J.; Tegenfeldt, J. O.; Austin, R. H.; Wu, W.;Chou, S. Y. *Appl. Phys. Lett.* 2002, *81*, 174–176.

4. Han, J.; Graighead, H. G. *Science* 2000, *288*, 1026–1029.
5. Dukkipati, V. R.; Pang, S. W. *Appl. Phys. Lett.* 2007, *90*, 083901.
6. Huh, D.; Mills, K. L.; Zhu, X.; Burns, M. A.; Thouless, M. D.;Takayama, S. *Nat. Mater.* 2007, *6*, 424–428.
7. Liang, X.; Morton, K. J.; Austin, R. H.; Chou, S. Y. *Nano Lett.* 2007,*7*, 3774–3780.

8. J. T. Mannion, H. G. Craighead
"Review: Nanofluidic structures for single biomolecule fluorescent detection,"
November 2006 in Wiley InterScience (www.interscience.wiley.com). DOI 10.1002/bip.20629

9, Mijatovic, D.; Eijkel, J. C. T.; van den Berg, A. *Lab Chip* 2005, *5*, 492–500.

10. Lei Zhang, Fuxing Gu, Limin Tong and Xuefeng Yin, **"**Simple and cost-effective fabrication of two-dimensional plastic nanochannels from silica nanowire templates,"
Microfluidics and Nanofluidics, Berlin / Heidelberg ISSN1613-4982 (Print) 1613-4990 (Online) IssueVolume 5, Number 6 / December, 2008 , DOI10.1007/s10404-008-0314-4 Pages727-732 , CollectionEngineering , June, 2008

11.Jeffrey L. Perry Æ Satish G. Kandlikar, "Review of fabrication of nanochannels for single phase liquid flow," Microfluid Nanofluid (2005), DOI 10.1007/s10404-005-00681
12. Xia, D.; Biswas, A.; Li, D.; Brueck, S. R. J. *Adv. Mater.* 2004, *16*, 1427 , "Introduction of Three-Dimensional Extrinsic Defects into Colloidal Photonic Crystals"
13. Xia, D.; Brueck, S. R. J. *Nano Lett.* 2004, 4, 1299, "DNA Transport in Hierarchically-Structured Colloidal-Nanoparticle Porous-Wall Nanochannels"
14. Xia, D., Gamble, T. C., Mendoza, E. A., Koch, S. J., He, X., Lopez, G. P., and Brueck, S. R. J., *Nano Lett.*, 2008, 8, 1617, "Strongly Anisotropic Wetting on One-Dimensional Nanopatterned Surfaces"

15. SwatiGoyal, Young-tae Kim, Samir M, "Effect of Fluorescent Tags on Translocation through

Nanochannels,' 32nd Annual International Conference of th IEEE EMBS, 2010

Patents

6,913,697 B2 G. P. Lopez, S. R. J. Brueck, and L. K. Ista, Nanostructured Separation and Analysis Devices for Biological Membranes,

RE41,762 G. P. Lopez, S. R. J. Brueck and L. K. Ista, Nanostructured Separation and Analysis Devices for Biological Membranes (issued 9/28/2010).

7,825,037 S. R. J. Brueck and Deying Xia, Fabrication of Enclosed Nanochannels using Silica Nanoparticles (provisional 10/17/2005; issued 11/2/2010)

RE42,249 Gabriel P. Lopez, S. R. J. Brueck and Linnea K. Ista, Nanostructured Separation and Analysis Devices for Biological Membranes, (reissued 3/29/2011).

RE42,315E Gabriel P. Lopez, S. R. J. Brueck and Linnea K. Ista, Nanostructured Separation and Analysis Devices for Biological Membranes, (reissued 5/3/2011).

7,959,861 G. P. Lopez, Linnea Ista, S. R. J. Brueck, A. E. Lara and M. Bore, Integrated Affinity Microcolumns and Affinity Capillary Electrophoresis (UNM 782 issued 6/14/2011).

8,105,471 Sang M. Han, Steven R. J. Brueck, Cornelius F. Ivory, Gabriel P. Lopez and Dimiter N. Petsev, Nanofluidics for bioseparation and analysis (issued 1/31/2012).